WILEY | eFood

**RESEARCH ARTICLE** OPEN ACCESS

# Almond Polysaccharide Ameliorates DSS-Induced Ulcerative Colitis in Mice by Restoring Intestinal Barrier Function and Modulating Gut Microbiota and SCFAs Metabolism

Yanqi Peng[1,2,3] | Ji Wu[1,3] | Ronghua Fan[1,3] | Mingyue Ma[1] | Xixin Wang[4] | Yuzhen Pi[2] | Xiqing Yue[2] | Yanyu Peng[3,5]

[1]School of Public Health, Shenyang Medical College, Shenyang, People's Republic of China | [2]College of Food Science, Shenyang Agricultural University, Shenyang, People's Republic of China | [3]Shenyang Key Laboratory of Chronic Disease Assessment and Nutritional Intervention for Heart and Brain, Shenyang Medical College, Shenyang, People's Republic of China | [4]Shenyang Medical College, Shenyang, People's Republic of China | [5]Department of Histology and Embryology, School of Basic Medicine, Shenyang Medical College, Shenyang, People's Republic of China

**Correspondence:** Yuzhen Pi (yuzhen_pi@sina.com) | Xiqing Yue (yxqsyau@126.com) | Yanyu Peng (yypeng@cmu.edu.cn)

## ABSTRACT

The development of new therapeutic strategies for ulcerative colitis (UC) requires the targeting of multiple pathogenic factors, including disruption of the colonic mucosal barrier, dysregulated inflammation, and gut microbiota imbalance. This study aimed to investigate the protective mechanisms of almond polysaccharide (AP1) against dextran sulfate sodium (DSS)-induced UC in mice. Administration of AP1 significantly restored DSS-induced reductions in goblet cells and inhibited epithelial apoptosis, thereby preserving colonic mucosal barrier integrity. In addition, AP1 decreased the levels of proinflammatory cytokines and oxidative stress markers in colonic tissues. Gut microbiota analysis revealed that AP1 effectively restored microbial composition and diversity. Furthermore, AP1 increased the relative abundance of beneficial bacteria while reducing pathogenic taxa, thereby contributing to the restoration of intestinal microbial balance in UC mice. Metabolomic analysis of short-chain fatty acids (SCFAs) demonstrated that DSS-induced UC significantly depleted major SCFAs (acetic acid, propionic acid, n-butyric acid) and disrupted branched-chain fatty acid (i-butyric acid and i-valeric acid) metabolism, whereas AP1 intervention reestablished SCFA profiles. Correlation analysis showed *Bacteroides* negatively correlated with multiple SCFAs, whereas *Alistipes* positively correlated with propionic acid. Collectively, these findings underscore the role of AP1 in rescuing microbiota-derived SCFA metabolism. In summary, AP1 was shown to alleviate UC symptoms through multiple mechanisms, including the preservation of mucosal barrier integrity, suppression of oxidative stress and inflammation, and modulation of gut microbiota composition and the intestinal microenvironment. These results support the therapeutic potential of AP1 as a natural polysaccharide-based agent for UC treatment.

# 1 | Introduction

Inflammatory bowel disease (IBD), including ulcerative colitis (UC) and Crohn's disease (CD), is characterized as chronic, relapsing gastrointestinal disorder. It is defined by dysregulated mucosal immunity and an imbalance between the host and its commensal microorganisms, and arises from a complex interaction of genetic, environmental, and microbiological factors (Graham and Xavier 2020). The rising prevalence of UC has been associated with an increased risk of colorectal cancer due to ongoing mucosal damage, thereby posing a significant global health burden (Beaugerie and Itzkowitz 2015; Gao et al. 2023). Current UC therapies are often empirical and remain limited by drug resistance and systemic toxicity, which underscores the need for novel, safer interventions targeting the mucosal barrier, inflammation, immune regulation, and microbial ecology (Graham and Xavier 2020).

Intestinal homeostasis is sustained through complex interactions among the intestinal epithelium, luminal antigens, immune cells, and the gut microbiota (X. Y. Guo et al. 2020; Walrath et al. 2021). Prolonged disruption of the intestinal barrier leads to increased exposure to bacterial antigens, thereby perpetuating chronic inflammation (Prame Kumar et al. 2023). Mucosal barrier dysfunction and microbial dysbiosis have been identified as central factors driving immune activation during the progression of IBD (van der Post et al. 2019; Paone and Cani 2020; Fang et al. 2021; Zou et al. 2021). The intestinal commensal microbiota plays a crucial role in modulating host immune responses by maintaining microbial equilibrium (Prame Kumar et al. 2023). Therefore, microbial diversity and homeostasis are essential for maintaining immune homeostasis in the host. In addition, an imbalance in metabolites and gut microbiota composition can compromise the immune response in the gut and further impair the intestinal barrier.

Oxidative stress plays a pivotal role in UC by causing colonic mucosa damage and triggering the release of proinflammatory mediators, including cytokines, interleukins, and chemokines (Tocmo et al. 2021; H. Zhang et al. 2023). Notably, activation of nuclear factor kappa B (NF-$\kappa$B) under oxidative stress results in excessive production of inflammatory mediators, such as TNF-$\alpha$ and COX-2, thereby contributing to sustained intestinal inflammation (Y.-E. Chen et al. 2021; M. Liu, Guan, et al. 2024). Our previous work demonstrated that almond polysaccharide (AP1) suppresses NF-$\kappa$B activation in both in vitro and in vivo models: in LPS-stimulated RAW264.7 macrophages, AP1 suppressed NO and ROS production and downregulated the expression of TNF-$\alpha$, IL-6, and COX-2 (Peng, Li, et al. 2024); in dextran sulfate sodium (DSS)-induced colitis mice, AP1 reduced colonic expression of NF-$\kappa$B-related inflammatory mediators and alleviated mucosal injury (Peng, Zhu, et al. 2024). Oxidative stress amplifies intestinal inflammation by promoting immune cell activation and the release of proinflammatory mediators. Therefore, effective control of oxidative stress is critical for limiting the release of proinflammatory cytokines and preventing further tissue injury.

Graham and Xavier (2020) suggested that, given the complex pathophysiology of IBD, natural polysaccharides may serve to modulate immunity, enhance barrier function, and reshape the microbiota, thereby showing potential as IBD treatments by intervening in the gut–immune–microbiota axis. In support of this view, recent studies have demonstrated the protective effects of different natural polysaccharides in DSS-induced colitis. *Dendrobium officinale* oligosaccharides (DOO) were found to alleviate colitis symptoms, suppress NF-$\kappa$B pathway activation, modulate gut microbiota composition, and increase short-chain fatty acid (SCFA) production, thus maintaining intestinal homeostasis (Shi et al. 2025). Likewise, *Lactobacillus acidophilus* 6074-fermented jujube juice (LAFJ) was shown to improve colitis outcomes by repairing intestinal barrier integrity, regulating proinflammatory cytokines, attenuating oxidative stress, and reshaping gut microbiota (H. Li, Fan, et al. 2025). These findings highlight that natural polysaccharides and polysaccharide-rich functional foods represent promising therapeutic strategies for UC. In our search for natural, safe, and effective treatments for colitis, AP1 isolated and purified from almond residues, was identified as a candidate due to its biological properties. AP1 is a neutral polysaccharide with minimal uronic acid content. Its monosaccharide composition consists predominantly of glucose, with trace amounts of arabinose and galactose, and the backbone is mainly composed of glucose units. The molecular weight distribution, determined by gel permeation chromatography (GPC), indicated that AP1 belongs to a moderate-molecular-weight fraction. These structural features have been reported in our previous studies (Peng et al. 2023; Peng, Li, et al. 2024; Peng, Zhu, et al. 2024), where AP1 was also shown to exhibit anti-inflammatory and prebiotic activities. AP1 has been observed to modulate the intestinal flora of healthy humans and effectively increases the relative abundance of *Lactobacillus* and *Bifidobacterium* (Peng et al. 2023; Peng, Li, et al. 2024; Peng, Zhu, et al. 2024). In addition, in LPS-induced RAW264.7 cells, AP1 exerts anti-inflammatory effects by reducing NO release, regulating ROS levels, and downregulating the expression of inflammatory cytokines (Peng, Li, et al. 2024). In our previous in vivo study (Peng, Zhu, et al. 2024), AP1 significantly reduced the DAI score in mice with DSS-induced UC and alleviated pathological damage to the colonic tissue. The first line of defense in the colonic tissue is provided by the mucus layer secreted by goblet cells on its surface. Thus, we hypothesized that AP1 would mitigate colonic pathological damage in DSS-induced UC mice by enhancing the integrity of the first-line colonic barrier, inhibiting inflammation progression, modulating microbiota homeostasis, and restoring SCFA levels. Therefore, we undertook a comprehensive analysis of changes in the mucosal layer, oxidative stress responses, gut microbiota, and metabolites in DSS-induced mice to elucidate the potential multi-target mechanism of AP1 in alleviating colitis and to establish links between its structural properties and biological activities.

# 2 | Methods

## 2.1 | Materials and Reagents

The almond residue was a by-product generated after the cold-pressing extraction of almond oil (supplied by Xinglinchunxiao Chengde Biotechnology Co. Ltd.). The extraction and purification procedure for the AP1 fraction from *Armeniaca sibirica* L. Lam. has been described in detail in our previous publications (Peng

et al. 2023; Peng, Li, et al. 2024). Briefly, dried almond residues were subjected to hot-water extraction, ethanol precipitation, and Sevag deproteinization, followed by purification using DEAE-52 cellulose ion-exchange chromatography and Sephadex G-100 gel filtration. The structural features of AP1—monosaccharide composition (predominantly glucose with trace arabinose and galactose), molecular weight distribution determined by GPC, and characteristic glycosidic linkages confirmed by FTIR and NMR—have also been reported in these studies, with overall purity > 95% verified by HPLC. DSS (molecular weight 36,000–50,000 Da; Batch No. 160110, MP Biomedicals, Irvine, CA, USA). The 30 male C57BL/6 mice (6–8 weeks old, 20–25 g), specific pathogen free (SPF grade), were obtained from Liaoning Changsheng Biotechnology Co. Ltd. (Liaoning, China; animal production license no.: SCXK (Liao) 2020-0001).

## 2.2 | Experimental Design

In this study, mice were raised in a strictly controlled environment (Peng, Zhu, et al. 2024). Specifically, the animals were housed under SPF conditions at 22 ± 2°C, with 50%–60% relative humidity, and a 12 h light/dark cycle, with free access to food and water. Randomization into groups was performed using a computer-generated random number sequence to ensure unbiased allocation. The entire experimental protocol was approved by the Experimental Animal Ethics Committee of Shenyang Agricultural University (Approval No. 2023052201). The mice were assigned randomly to six different treatment groups: (control group), DSS-induced model group (DSS group), other three groups were preventive treatment groups: DSS + low dose AP1 group (DSS + AP1–L group, 100 mg/g day), DSS + medium dose AP1 group (DSS + AP1–M group, 200 mg/kg day), and DSS + high dose AP1 group (DSS + AP1–H group, 500 mg/kg day). In addition, 5-aminosalicylic acid (5-ASA) was administered to a positive control group (5-ASA group) ($n = 5$ per group). The experimental groups and dosage concentrations were consistent with the results of our previous experiments (Peng, Zhu, et al. 2024). The AP1 dosage and concentration groups used in all experiments in this study were based on the results of our previous experiments. Apart from the control group, the rest of the groups were continuously administered free 3% DSS liquid (w/v) to induce UC according to a previously described method (Peng, Zhu, et al. 2024). The control group was administered the same amount of water daily as the treated groups. Meanwhile, the AP1 treatment groups were administered different doses of AP1 (low, medium, and high) daily for 8 days. The 5-ASA treatment group was administered 100 mg/kg of 5-ASA for 8 days daily. After that, the mice were sacrificed under anesthesia. Colon tissues and spleens were gathered for the following experiments.

## 2.3 | Histologic Analysis and Periodic Acid–Schiff Staining

Following washing of the colon with stored sterile saline, approximately 1 cm of mid-colonic tissue was cut-off and fixed in 4% paraformaldehyde. Dehydration, embedding and sectioning were performed on the fixed colon tissues. Periodic acid–Schiff (PAS) (WL033a, Wanleibio, China) and hematoxylin–eosin (HE) (Cat No. C0105, Beyotime Biotechnology, Shanghai, China) staining

were performed to observe morphological differences of the five treatment groups. A light microscope (Olympus, Japan) was used to photograph the staining results.

## 2.4 | TdT-Mediated dUTP Nick-End Labeling Assay

Paraffin-embedded distal sections of the colon were deparaffinized and immersed in citrate buffer (pH 6.0) containing 0.1% Triton X-100, then incubated with TdT-mediated dUTP Nick-End Labeling (TUNEL) dye liquor (Cat No. WLA127a, Wanleibio), sealed from light with anti-fluorescence sealant (containing DAPI) (Cat. No.: D106471-5 mg, Aladdin, China). The quantitative analysis of TUNEL-positive signals was performed using ImageJ software (NIH). The apoptosis index was calculated by normalizing the TUNEL-positive area to the total nuclear area in each region.

## 2.5 | Analysis of Reverse Transcription-Quantitative Polymerase Chain Reaction

Total RNA was extracted from colonic tissues using a TRIpure (Cat. No. RP1001, BioTeke, China) and stored at −80°C. cDNA was synthesized using the BeyoRT II Moloney Murine Leukemia Virus reverse transcription kit (Cat. No. D7160L, Beyotime Biotechnology, China). Then, reverse transcription-quantitative polymerase chain reaction (RT-qPCR) amplification was performed on the 2X Taq PCR MasterMix Kit (Cat. No. PC1150, Solarbio, China) following the manufacturer's instructions. The expression of the genes was normalized to that of $\beta$-actin and calculated using the $2^{-\Delta\Delta C_t}$ method. Primers for the target genes, including IL-1$\beta$ and TNF-$\alpha$, were synthesized by BioTeke Co. Ltd. (Beijing, China). The primer sequences were as follows (species, mouse): IL-1$\beta$: forward AGCATCCAGCTTCAAATC,

IL-1$\beta$: reverse ATCTCGGAGCCTGTAGTG;

TNF-$\alpha$: forward TTCTCATTCCTGCTTGTGG,

TNF-$\alpha$: reverse CACTTGGTGGTTTGCTACG;

$\beta$-actin: forward CATCCGTAAAGACCTCTATGCC,

$\beta$-actin: reverse ATGGAGCCACCGATCCACA.

RT-qPCR was conducted by using the Exicycler 96 machine (BIONEER, Korea).

## 2.6 | Inflammatory Cytokines and Antioxidant Measurement

The samples of colon were taken for the extraction of protein and then the protein levels of MDA (Cat. No. WLA048, Wanleibio), CAT (Cat. No. A007, Jiancheng Bio, China), and IL-18 enzyme-linked immunosorbent assay (ELISA) kit (Cat. No. EK218, Liankebio, China) were detected using a BCA protein assay kit (Cat. No. WLA004, Wanleibio) following the instruction.

## 2.7 | Profiling of the Gut Microbiota by 16S rRNA Sequencing and Bioinformatics Analysis

Total bacterial DNA was extracted from fecal samples using the FastDNA SPIN DNA kit (MP Biomedicals). The DNA extract quality was assessed by 1% agarose gel electrophoresis. DNA purity and concentration were measured by a NanoDrop 2000 spectrophotometer (Thermo Fisher, USA). The V3–V4 region of the 16S rDNA gene was amplified with the primers 338F: (5′-ACTCCTACGGGAGGCAGCAG-3′) and 806R (5′-GGACTACHVGGGTWTCTAAT-3′) (produced by Allwegene Tech, China). Amplification results were further analyzed by 2% agarose gel electrophoresis, where fragments of interest were excised and subsequently recovered using the Agencourt AMPure X DNA Gel Recovery Kit (Beckman Coulter, USA). The Illumina MiSeq platform (Illumina Inc., CA) was used to sequence the amplicons. QIIME software was applied to calculate both alpha ($\alpha$) diversity indices and beta ($\beta$) diversity indices. To analyze the gut microbiota in the different groups, linear discriminant analysis (LDA) and LDA effect size (LEfSe) methods were used, with a logarithmic score threshold of 3.5 for LDA analysis. Graphical representations were generated using the Personalbio analysis platform (https://www.genescloud.cn/).

## 2.8 | Fecal SCFA Analysis

Analysis of fecal SCFAs was carried out as reported previously (Han et al. 2018; Hsu et al. 2019; S. Zhang et al. 2019). Stool samples were collected and stored at −80°C until assayed. In brief, fecal samples were homogenized with 500 µL water and 100 mg glass beads for 1 min using a high-throughput tissue grinder, followed by centrifugation at 12,000 rpm (4°C, 10 min). A 200 µL supernatant aliquot was acidified with 100 µL 15% phosphoric acid, spiked with 20 µL 375 µg/mL 4-methylvaleric acid (internal standard), and extracted with 280 µL ether. After vortexing (1 min) and centrifugation (12,000 rpm, 4°C, 10 min), the ether layer was transferred to GC–MS vials. Analysis used a Trace 1310 GC-ISQ 7000 MS system (Thermo Fisher Scientific Inc., Waltham, MA, USA) with an HP-INNOWAX column (30 m × 0.25 mm × 0.25 µm). Helium carrier gas flowed at 1.0 mL/min with split injection (10:1, 250°C, 1 µL). Oven program: 90°C → 120°C (10°C/min) → 150°C (5°C/min) → 250°C (25°C/min, hold 2 min). MS detection used EI (70 eV) in SIM mode with ion source/transfer line at 300°C/250°C. The concentration of SCFAs was converted to micromoles per gram (van der Lelie et al. 2021).

## 2.9 | Statistical Analyses

SPSS version 22.0 was used for data processing, with results presented as mean ± standard deviation (SD) derived from at least three independent in vitro or six mice per group in vivo. Tukey's multiple comparison tests used one-way analysis of variance (ANOVA), and two-tailed Student's $t$ tests were used for comparisons between two groups. Tukey's multiple comparison tests used one-way ANOVA. Correlation analysis used Spearman's analysis. $*p < 0.05$; $**p < 0.01$; $***p < 0.001$ was considered a statistically significant difference. The ns means no significance.

## 3 | Results

### 3.1 | AP1 Reverses Goblet Cell Reduction and Suppresses Epithelial Cell Apoptosis in DSS-Induced Colitis

The DSS-induced colitis model in mice is the most commonly used chemically induced model for studying intestinal inflammation. In DSS-induced colitis mice, we first observed the effects of AP1 on the colonic mucosal epithelium. The first line of defense in the intestinal mucosa is provided by goblet cells, which secrete mucus to protect epithelial cells from damage. PAS staining was used to quantify the number of goblet cells in the colonic mucosa. Compared to the control group, DSS-induced mice had fewer goblet cells, reduced mucus secretion, and varying degrees of epithelial desquamation (Figure 1a). Pathological changes in the colonic tissues of the AP1 treatment groups at different doses showed significant alleviation compared to the DSS model group. A dose-dependent increase in goblet cell numbers was observed in the AP1 treatment groups with increasing AP1 concentrations. Epithelial cell apoptosis in the mucosa was detected using the fluorescent TUNEL method. Fluorescence analysis revealed a significant increase in apoptotic cells in both the DSS model and AP1 treatment groups compared to the control group (Figure 1b). In the AP1–L group, apoptosis rates were higher than in the medium and high-dose groups. These results suggest that DSS can destroy mouse mucosal goblet cells and induce apoptosis, with AP1 showing a weaker inhibitory effect on mucosal cell apoptosis.

Thus, the increase in goblet cell numbers may not be directly related to the reduction in apoptosis, but AP1 intervention can reduce pathological damage and provide a specific protective effect for UC mice colonic tissues.

### 3.2 | AP1 Alleviates DSS-Induced Inflammatory Response in Colitis Mice Through Immune Activation and Antioxidative Stress

When intestinal immune function was compromised, a systemic immune response was triggered. We aimed to indirectly assess the systemic immune response by observing the spleen and directly evaluate local immune inflammation in colon tissue by measuring inflammatory cytokines. As shown in Figure 2a, spleen weight was significantly higher in the DSS-induced model group compared to controls. Spleen weights were significantly lower in all AP1-treated groups compared to the DSS model group. Notably, the reduction in spleen weight in AP1 treatment groups was dose dependent. No significant difference was found between the high-dose AP1 and positive 5-ASA treatment groups. Therefore, AP1 may attenuate systemic immune responses.

To evaluate AP1's anti-inflammatory effects, we measured inflammatory cytokine levels in local colon tissue. First, IL-1$\beta$ and TNF-$\alpha$ levels in colon tissue were significantly higher in DSS-induced mice compared to controls. All AP1 treatment groups showed a significant decrease in IL-1$\beta$ levels compared to the DSS model group. However, only the AP1–M and AP1–H treatment groups showed significant differences in TNF-$\alpha$ levels compared to the DSS model group. Levels decreased with increasing AP1 concentrations in a dose-dependent manner, but
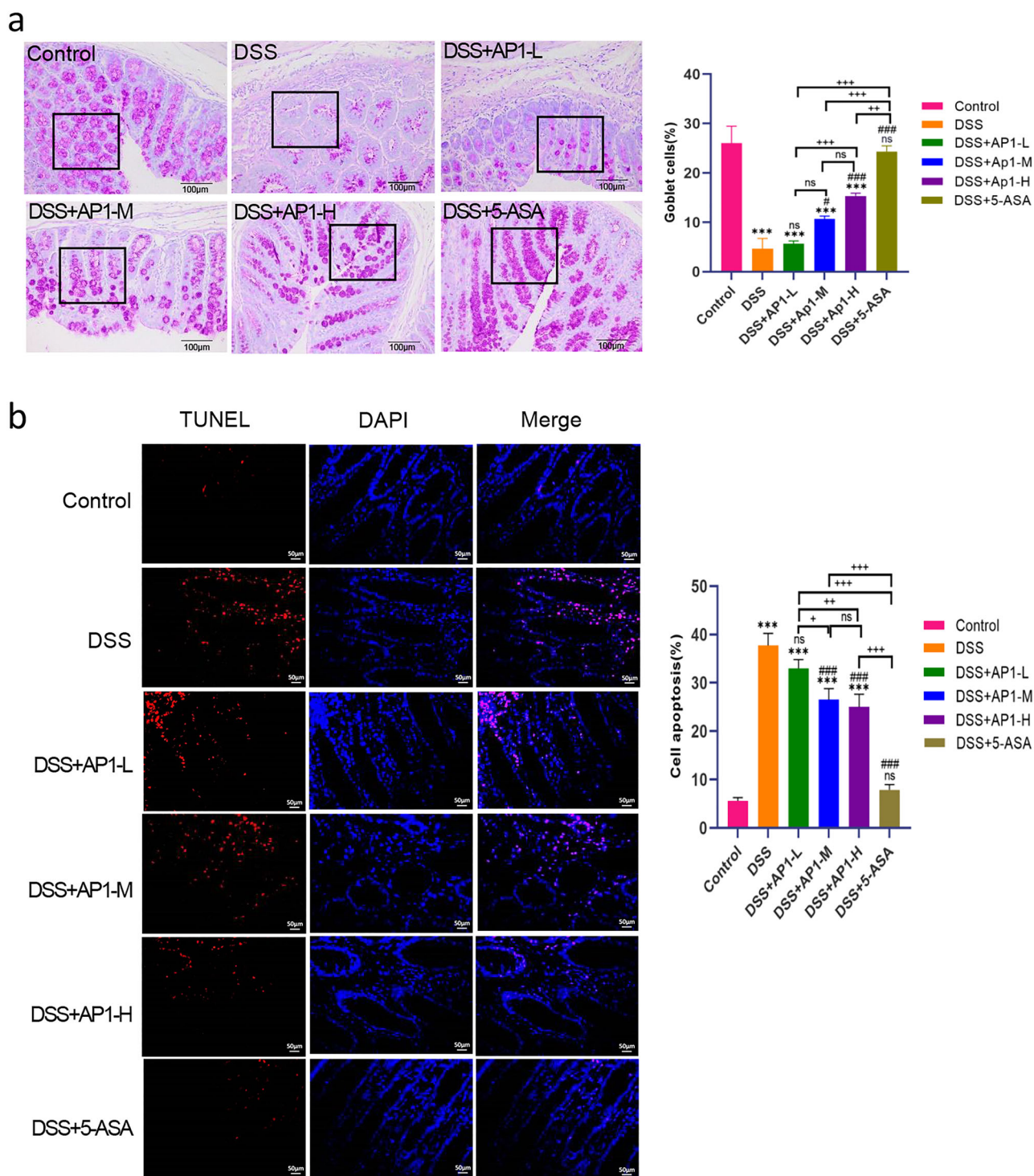
**FIGURE 1** | Effect of AP1 on reduction of goblet cells and epithelial cell apoptosis. (a) PAS staining image and count ratio of colonic tissues in different groups (magnification, 200×). (b) Representative TUNEL staining image of colon tissues in different groups (magnification, 400×). Scale bar = 100 μm. Data were expressed as mean ± SD. *$p < 0.05$, **$p < 0.01$, ***$p < 0.001$ versus control group. #$p < 0.05$, ##$p < 0.01$, ###$p < 0.001$ versus DSS group.

no statistically significant differences were observed between the medium and high-dose groups. TNF-$\alpha$ expression followed a similar dose-dependent trend as IL-1$\beta$, with no statistically significant differences between the low and medium-dose groups. Importantly, no significant differences were found for either IL-1$\beta$ or TNF-$\alpha$ between the high-dose and positive 5-ASA groups. This suggests that AP1 treatment restored the DSS-induced increase in IL-1$\beta$ and TNF-$\alpha$ levels, with the anti-inflammatory effects of the AP1–H group comparable to those of the positive control drug (Figure 2b,c).
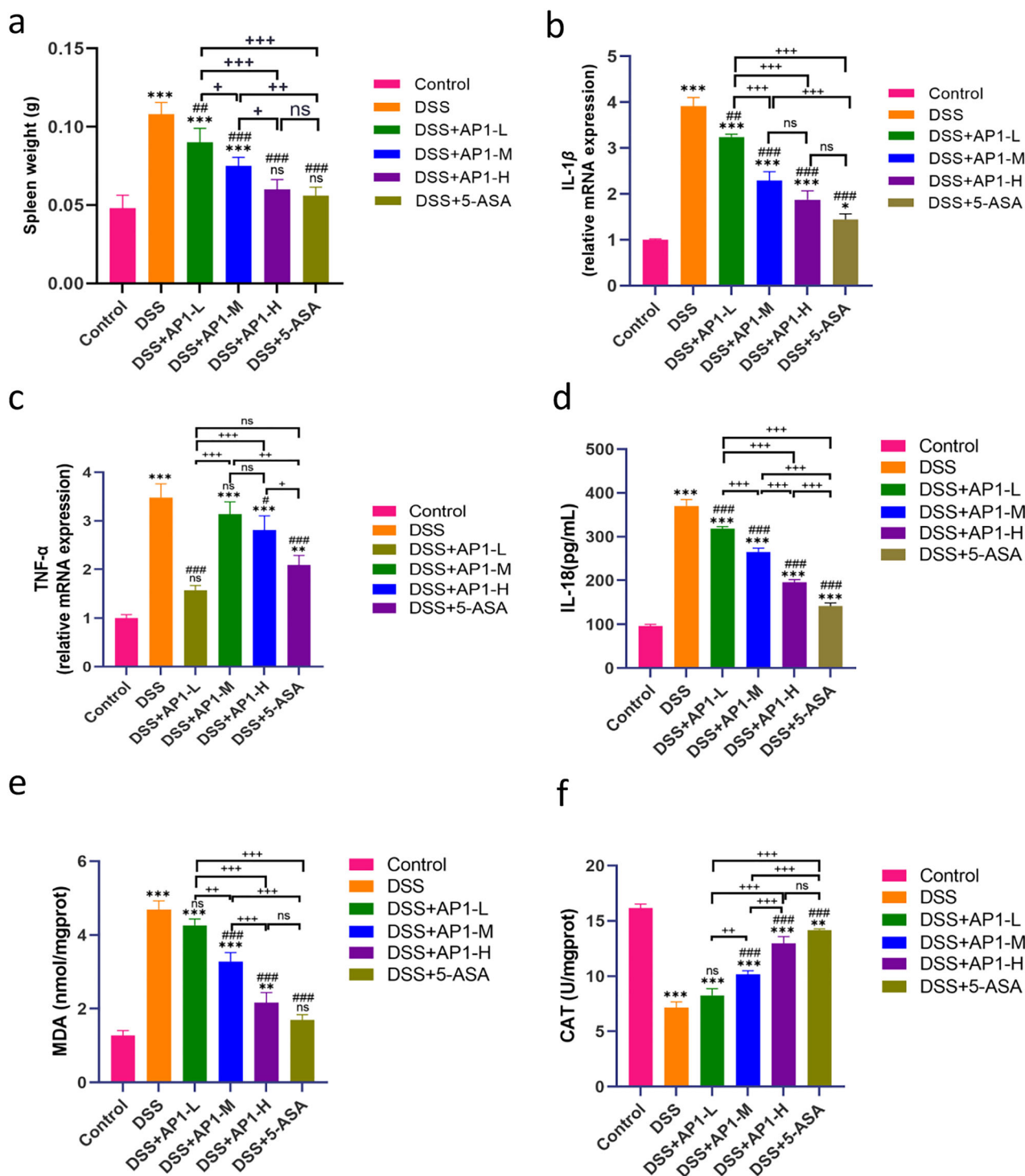
**FIGURE 2** | AP1-influenced inflammatory cytokines and oxidative stress biomarkers in DSS-induced colitis mice. (a) Spleen weight. RT-qPCR analyzed the relative expression of (b) IL-1$\beta$ and (c) TNF-$\alpha$. (d) ELISA determined IL-18 levels. The expression of (e) MDA levels and (f) CAT activity in the colon. Data are expressed as mean ± SD. *$p < 0.05$, **$p < 0.01$, ***$p < 0.001$ versus control group. #$p < 0.05$, $p < 0.01$, $p < 0.001$ versus DSS group.

IL-18 levels in the colon tissues of colitis mice were subsequently measured by ELISA (Figure 2d). After treatment with different doses of AP1, IL-18 levels in the AP1-treated mice were significantly lower than in the DSS model group. MDA, a free radical-mediated product of lipid peroxidation, indirectly reflects the severity of cellular damage. Lower antioxidative enzyme levels are associated with greater oxidative stress-induced cellular

damage (Kaviani et al. 2017; Z. Li et al. 2020; Zheng et al. 2024). We next assessed oxidative stress levels in the colonic tissues of UC mice. The results showed that, compared to the control group, MDA activity (Figure 2e) was significantly higher and CAT activity (Figure 2f) was significantly lower in the DSS model group. This suggests that mice in the DSS model group were undergoing oxidative stress. MDA activity was downregulated

and CAT activity upregulated in the AP1–M and AP1–H groups, with no significant difference in MDA levels between the DSS and AP1–L groups. In the high-dose AP1 treatment group, CAT and MDA expression levels were not significantly different from those in the positive 5-ASA treatment group (Figure 2e,f). Thus, the antioxidant action of AP1 may be mediated by downregulating MDA and upregulating CAT.

In summary, AP1 alleviates colonic injury in UC mice by reducing oxidative stress and inhibiting inflammatory cytokines.

## 3.3 | AP1 Effects on the Gut Microbiota in DSS-Induced Colitis Mice

We examined colonic contents using the V3–V4 region of 16S rRNA to determine whether AP1 could influence gut microbial composition and alleviate colitis. Venn diagrams were used to display OTUs that were unique and shared between different groups based on the OTU clustering results. As shown in Figure 3a, the Venn diagram revealed that all groups shared 240 species, considered the core microbiota. The control group had 29 unique species, while the DSS and DSS + ASA groups had three and two unique species, respectively. The DSS + AP1–L, DSS + AP1–M, and DSS + AP1–H groups showed 10, 10, and 11 unique species, respectively. AP1 can modulate the gut microbiota in UC mice, although different doses of AP1 had minimal effects on OTU composition.

We next assessed the effects of AP1 on gut microbiota composition and analyzed changes in microbiota abundance at the phylum, family, and genus levels across different treatment groups. Figure 3b presents the differences in gut microbiota abundance between groups at the phylum level, showing the top 10 representative phyla. Our results showed that *Bacteroidetes*, *Firmicutes*, and *Proteobacteria* had higher relative abundances in the samples. Specifically, the abundance of *Bacteroidetes* and *Proteobacteria* was higher in the DSS model colitis mice group compared to controls, while *Firmicutes* was reduced. These results suggest a disrupted homeostasis of the gut microbiota in DSS-induced colitis mice. In addition, the AP1-treated groups showed a decrease in *Bacteroidetes* abundance and an increase in *Firmicutes* abundance compared to the DSS group. Notably, this increase in *Firmicutes* was dose dependent. This suggests that AP1 intervention may help restore homeostasis in the gut microbiota of UC mice.

We then focused on abundance trends at the family and genus levels. At the family level, *Bacteroidaceae*, *Enterobacteriaceae*, *Prevotellaceae*, *Erysipelotrichaceae*, *Tannerellaceae*, and *Burkholderiaceae* had increased abundance in the DSS-induced group compared to the control group. *Muribaculaceae*, *Lachnospiraceae, Lactobacillaceae*, *Rikenellaceae*, *Desulfovibrionaceae*, *Helicobacteraceae*, and *Marinifilaceae* had significantly decreased abundance in the DSS-treated group. This indicates that the distribution of gut microbiota was altered considerably at the family level. Next, the detailed study showed that the AP1-treated groups increased the relative abundance of *Lachnospiraceae*, *Prevotellaceae*, *Akkermansiaceae*, *Erysipelotrichaceae*, *Rikenellaceae*, and *Desulfovibrionaceae*, while decreasing the relative abundance of *Bacteroidaceae* and *Tannerellaceae* in comparison with

DSS-treated groups. These findings suggest that AP1 treatment could correct DSS-induced disturbances in the gut microbiota, thereby restoring a favorable gastrointestinal state. Furthermore, the relative abundances of *Marinifilaceae*, *Bacteroidaceae*, *Lachnospiraceae*, *Tannerellaceae*, and *Desulfovibrionaceae* were restored in a dose-dependent way with AP1. Compared to the 5-ASA treatment group, the AP1–H group exhibited nearly complete restoration of *Muribaculaceae*, *Bacteroidaceae*, *Tannerellaceae*, *Desulfovibrionaceae*, and *Helicobacteraceae* levels, similar to those in control subjects (Figure 3c).

At the genus level, differences in the abundance of 15 genera between the control and treatment groups are shown (Figure 3d). The respective abundance of *Bacteroides*, *Escherichia–Shigella*, *Parabacteroides*, *Parasutterella* showed a significant increase, and the *Lachnospiraceae* NK4A136 group, *Lactobacillus*, *Alistipes*, *Prevotellaceae* UCG-001, and *Helicobacter* abundances were decreased in the DSS model group in comparison with the control group. After AP1 intervention, the abundance of *Escherichia–Shigella*, *Lachnospiraceae* NK4A136 group, *Akkermansia*, and *Alloprevotella* was markedly increased, and the abundance of *Bacteroides* and *Parasutterella* was dramatically decreased compared to the DSS-treated group. Detailed analysis showed that the abundance of *Parabacteroides* and *Parasutterella* in AP1-treated groups was dose dependent. These results suggest that AP1 can restore the balance of gut microbiota in DSS-induced colitis mice.

A clustered heatmap was generated to assess the bacterial genus composition between DSS and AP1-treated groups. Figure 3e shows the relative abundance of each bacterial genus across samples. Color variations in this figure represent the relative abundance of each genus. It was found that the *Bacteroides*, *Paraprevotella*, and *Parabacteroides* were the most abundant genus compared to the control group in the DSS group samples. In contrast, *Candidatus Saccharimonas*, *Odoribacter*, *Ruminiclostridium 9*, *Lactobacillus*, and *Lachnospiraceae* NK4A136 group exhibited a notable decrease in the samples of the DSS group. The DSS model of colitis mice showed a higher abundance of harmful bacteria compared to the control group. In contrast, the characteristic beneficial bacteria were markedly increased and clustered in the AP1 intervention groups in comparison to the DSS group, including *Erysipelatoclostridium*, *Akkermansia*, *Prevotellaceae* UCG-001, *Prevotella 1*, *Ruminococcaceae* UCG-014, *Alloprevotella*, *Lachnospiraceae* NK4A136 group, *Helicobacter*, *Ruminiclostridium 9*, and *Alistipes*. The abundance of harmful bacteria was greater in DSS model colitis mice than in AP1-treated mice, while beneficial bacteria were less abundant. These results suggest that AP1 treatment led to notable changes in bacterial abundance at the genus level and restored the balance between beneficial and harmful bacteria.

## 3.4 | Analysis of the Diversity of the Gut Microbiota

We generated species accumulation curves based on OTUs from each sample at different sequencing depths (Figure 4a). The species count increased with the number of samples, and the smooth curve indicated that the sample size was adequate. This study confirmed that the sequencing sample size met the data analysis requirements. We applied $\alpha$ diversity to assess the
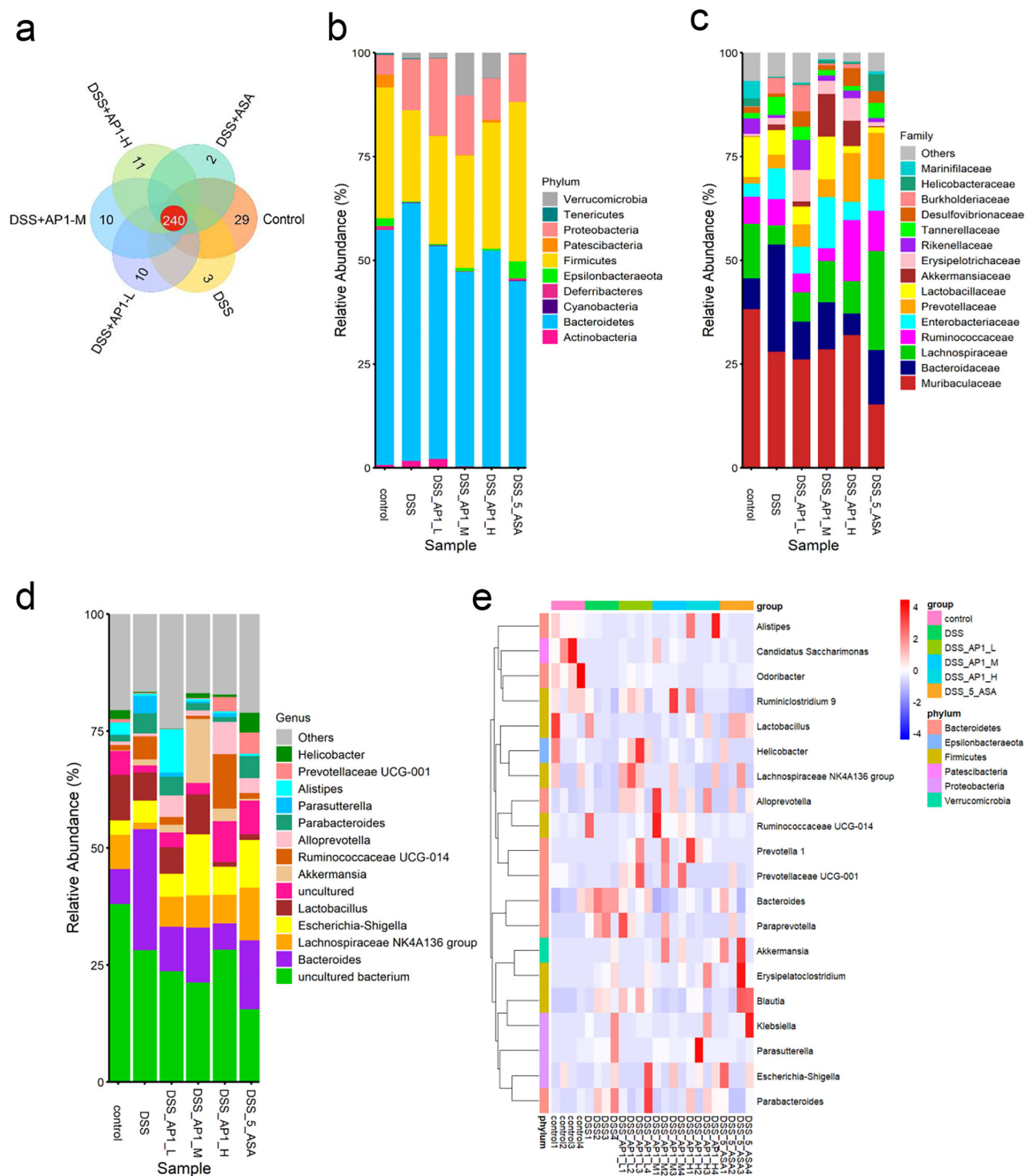
**FIGURE 3** | Effects of AP1 on the phylum family and genus levels of the gut microbiota. (a) Venn diagrams: species taxonomy OTUs, (b) phylum level, (c) family level, (d) genus level, (e) relative abundance of each bacterial genus using heat map analysis.

number of gut microbiota species and their relative abundances, reflecting the complexity and diversity of the microbiota. The coverage indices from the groups were above 0.999 (Figure 4b), indicating optimal sequencing reliability and integrity. The Chao1 and Shannon indices were significantly reduced in the DSS-induced model group compared to the control group. This finding suggests that the DSS-induced model group exhibited decreased gut microbiota diversity. AP1 intervention increased

both indices in DSS-induced colitis mice, particularly at the high dose, compared to the DSS-induced group (Figure 4c,d). These results suggest that AP1 treatment can effectively ameliorate DSS-induced gut microbiota disruption and restore balance.

To further assess gut microbiota composition, principal coordinate analysis (PCoA) was used to compare differences between individual samples. Figure 4e shows that PCoA revealed a clear
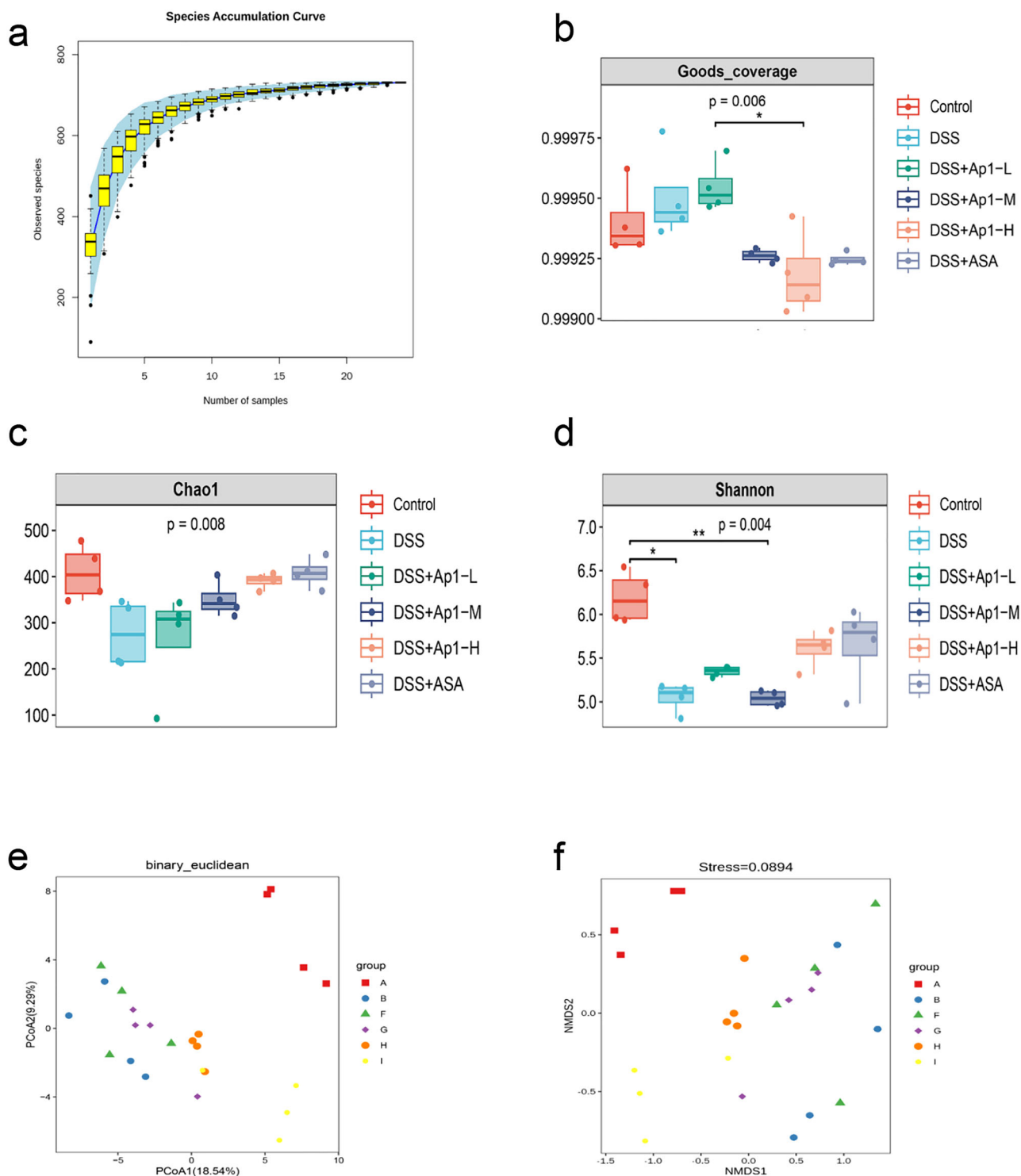
**FIGURE 4** | Analysis of the $\alpha$-diversity index of gut microbiota in DSS-induced colitis mice by AP1 treatment. (a) Species accumulation curve analysis. (b) Good coverage index analysis. (c) Chao1 index analysis. (d) Shannon index analysis. (e) Principal coordinates analysis. (f) Nonmetric multidimensional scaling analysis. In e and f: A, control; B, DSS; F, DSS + AP1–L; G, DSS + AP1–M; H, DSS + AP1–H; I, DSS + 5-ASA; keep consistent with the groups in other figures.

distinction in microbial community composition at the OTU level. The first and second principal coordinates accounted for 18.54% and 9.29% of the total variance, respectively. Notably, all groups of DSS-induced colitis mice exhibited clear separation from the control group in terms of gut microbiota. The gut microbiota of the AP1 treatment groups was more similar to

that of the control group than that of the DSS-induced model group. Furthermore, the distance between the AP1 intervention treatment groups at different doses and the DSS model group showed a dose-dependent ranking. The above results indicated that AP1 affected restoring dysbiosis in mice with DSS-induced colitis. In addition, nonmetric multidimensional scaling (NMDS)

analysis was performed at the OTU level. The analysis utilized a non-linear model based on the Bray–Curtis distance. The NMDS results (Figure 4f) were consistent with the PCoA analysis, showing differences between sample groups. We observed substantial separation between the DSS model group and the control group, with AP1-treated groups showing considerable separation from the DSS model group. Notably, AP1–H group samples were closer to the control group. This finding suggests minimal differences in overall gut microbiota composition between AP1–H and control groups.

LEfSe analysis revealed the gut-specific bacterial taxa with the most significant contribution from phylum to genus in each group. This was shown in Figure 5a,b. An LDA score threshold of 3.5 was used to screen for microorganisms that were highly abundant within their respective represented groups. The result indicated that at the genus level, the high abundance was *Odoribacter*, *Candidatus Saccharimonas*, and *Rikenella* in the control group; *Bacteroides*, *Parasutterella*, and *Paraprevotella* in the DSS-induced group; *Catenibacterium* in the AP1–L group; *Enterobacter* and *Acinetobacter* in the AP1–M group; *Dubosiella* in the AP1–H group; *Helicobacter* and *Ruminiclostridium 9* in the 5-ASA treatment group, respectively. In summary, AP1 treatment had a potential effect on the gut microbiota of colitis mice.

## 3.5 | Analysis of SCFAs

As shown in Table 1, in the control group, the concentrations of all SCFAs components were at high levels, with acetic acid (41.40 ± 14.12 µmol/g), propionic acid (5.86 ± 1.97 µmol/g), and n-butyric acid (12.14 ± 5.73 µmol/g) being the main components. Compared to the control group, SCFA concentrations in the DSS model group were significantly reduced. Specifically, acetic acid (7.05 ± 5.06 µmol/g), propionic acid (0.46 ± 0.54 µmol/g), and n-butyric acid (0.52 ± 0.52 µmol/g) decreased by 83.0%, 92.1%, and 95.7%, respectively ($p < 0.05$), suggesting impaired intestinal microbiota metabolic function. In addition, acetic acid, propionic acid, and n-butyric acid were 72.3%, 85.2%, and 88.1% lower than the mean values in the AP1 intervention group ($p < 0.05$), indicating significant metabolic inhibition in the DSS group and a marked impairment in the acid-producing capacity of the gut microbiota under inflammatory conditions. Compared to the DSS group, SCFA composition (except caproic acid) differed significantly between the DSS and AP1 intervention groups ($p < 0.05$). The highest fold increases were observed for n-butyric acid (831% in the AP1–M group) and propionic acid (1087% in the AP1–H group), suggesting that AP1 intervention significantly reverses DSS-induced SCFA depletion. Caproic acid concentrations were abnormally elevated in the DSS group but significantly decreased (by 76.9%–84.6%) after AP1 intervention, suggesting that its metabolism is linked to inflammation. Among the different AP1 intervention groups, the AP1–M group showed restoration effects of 9.3- and 4.5-fold compared to the DSS group for n-butyric acid (4.84 ± 0.38 µmol/g) and acetic acid (31.83 ± 2.47 µmol/g), respectively. In comparison, the AP1–H group showed restoration of i-butyric acid (0.29 ± 0.15 µmol/g) and i-valeric acid (0.19 ± 0.10 µmol/g) that were close to the control group levels ($p > 0.05$). Among major SCFAs such as acetic acid, propionic acid, and n-butyric acid, there were no significant differences between the AP1–M and AP1–H groups

TABLE 1 | Fecal SCFAs concentrations.

| Sample | Acetic acid | Propionic acid | i-Butyric acid | SCFAs (µmol/g) n-Butyric acid | i-Valeric acid | n-Valeric acid | Caproic acid |
|---|---|---|---|---|---|---|---|
| Con | 41.40 ± 14.12[b] | 5.86 ± 1.97[b] | 0.33 ± 0.16[ab] | 12.14 ± 5.73[a] | 0.17 ± 0.06[bc] | 0.22 ± 0.23[b] | 0.007 ± 0.005[ab] |
| DSS | 7.05 ± 5.06[e] | 0.46 ± 0.54[d] | 0.03 ± 0.04[d] | 0.52 ± 0.52[d] | 0.04 ± 0.05[d] | 0.028 ± 0.05[c] | 0.013 ± 0.013[a] |
| AP-L | 16.50 ± 3.32[d] | 3.66 ± 0.84[c] | 0.17 ± 0.034[c] | 2.61 ± 1.02[cd] | 0.10 ± 0.03[cd] | 0.17 ± 0.06[b] | 0.002 ± 0.0003[b] |
| AP-M | 31.83 ± 2.47[c] | 5.46 ± 0.47[b] | 0.21 ± 0.018[bc] | 4.84 ± 0.38[c] | 0.13 ± 0.01[bc] | 0.27 ± 0.03[b] | 0.003 ± 0.0009[b] |
| AP-H | 29.56 ± 5.08[c] | 5.53 ± 1.54[b] | 0.29 ± 0.15[abc] | 4.28 ± 1.01[c] | 0.19 ± 0.10[b] | 0.28 ± 0.08[b] | 0.002 ± 0.001[b] |
| 5-ASA | 52.02 ± 2.03[a] | 9.02 ± 0.69[a] | 0.4074 ± 03512[a] | 8.18 ± 0.65[b] | 0.28 ± 0.03[a] | 0.51 ± 0.05[a] | 0.004 ± 0.001[b] |

*Note*: The same lower case letters indicate significant differences ($p < 0.05$) between different groups.
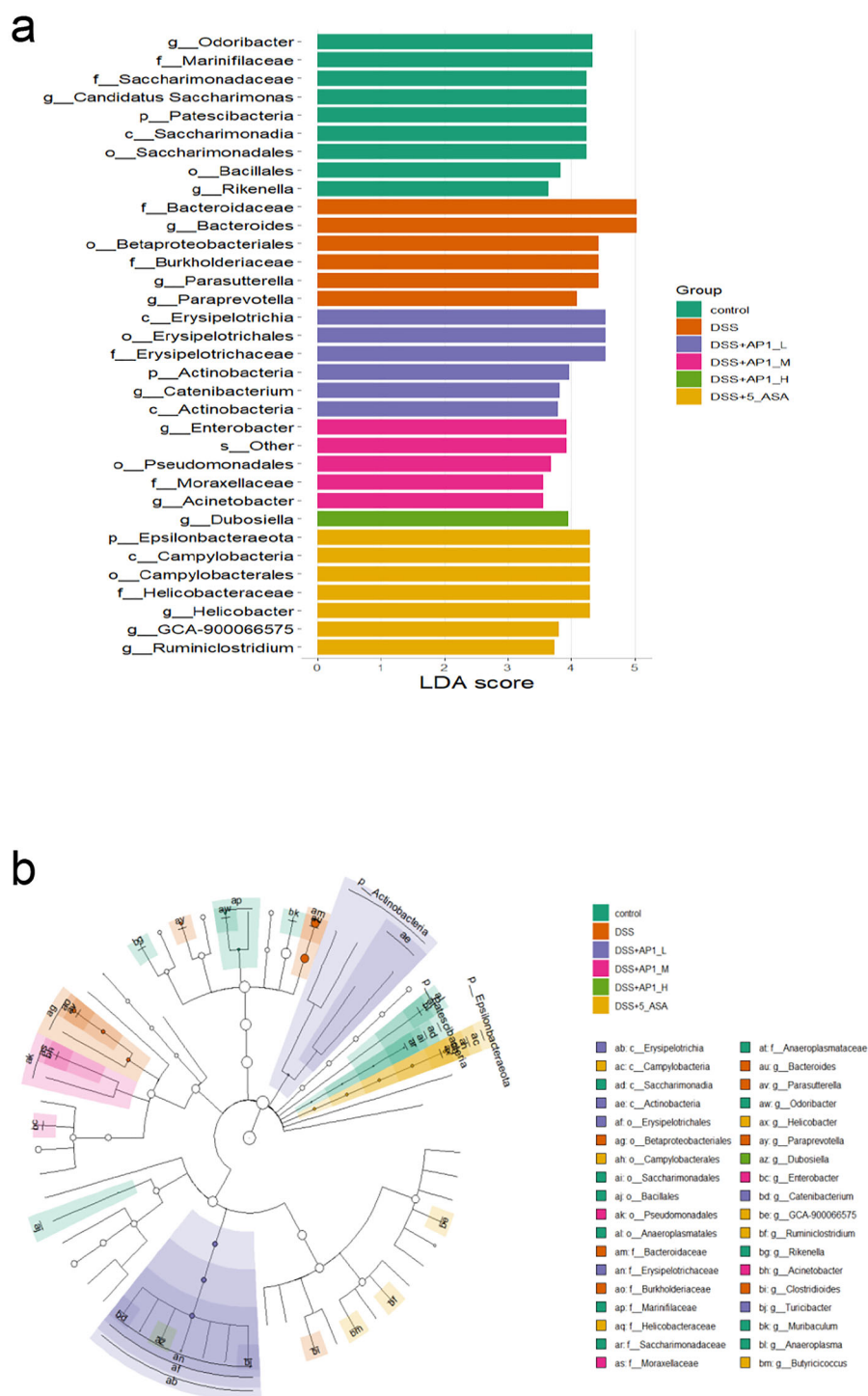
**FIGURE 5** | Linear discriminant analysis (LDA) and LDA effect size (LefSe) analysis. (a) LEfSe displayed by a histogram of LDA value distribution. (b) Evolutionary branching diagram of LEfSe analysis.

($p > 0.05$), but both were significantly higher than the AP1–L group. This suggested that the AP1–M might be the optimal dose for restoring major SCFAs. For i-butyric acid and i-valeric acid, the AP1–H group showed a dose-dependent increase compared to the AP1–M group, indicating a more significant effect on regulating branched-chain fatty acid (BCFA) metabolism. The AP1–L group only showed increased concentrations of acetic acid

and propionic acid compared to the DSS group, suggesting that AP1 intervention at low doses did not achieve effective regulatory concentrations. Caproic acid concentrations in the DSS group ($0.013 \pm 0.013$ μmol/g) were significantly higher than in all AP1 intervention groups ($p < 0.05$), and increasing AP1 doses did not affect its concentration. This suggested that caproic acid might serve as a specific metabolic marker of inflammation. Thus,

AP1 intervention dose dependently reversed DSS-induced SCFA depletion: AP1–M and AP1–H restored major SCFAs (acetic acid, propionic acid, n-butyric acid) to similar levels, whereas AP1–H exerted a stronger effect on BCFAs (i-butyric acid, i-valeric acid), and AP1–L had limited efficacy.

We next performed a cluster analysis of all targeted metabolites. Hierarchical clustering was used to cluster both samples and metabolites. The heatmap (Figure 6a) showed apparent clustering of differential metabolites, with consistent relative content in the AP1 treatment group samples. Furthermore, Figure 6b,c showed the results of the orthogonal partial least squares discriminant analysis (OPLS-DA) between the DSS-induced group and the medium- and high-dose groups. Mice treated with AP1–M and AP1–H were separated from the DSS model group. Furthermore, Figure 6d–k,l–s showed the relative content and correlation analysis of differential metabolites between the AP1–M group and the DSS model group, and the AP1–H group and the DSS model group. This revealed significant differences in SCFA content and consistent variation in metabolites between the AP1 treatment groups and the DSS model groups in UC mice. Finally, we used a metabolite molecular network map to analyze the metabolic pathways. As shown in Figure 7a, the main SCFA metabolic pathways were enriched in the degradation of aromatic compounds, protein digestion and absorption, propanoate metabolism, and carbohydrate digestion and absorption. Finally, the correlation analysis of gut microbial genus-level and SCFAs was conducted. As shown in Figure 7b, the relative abundance of *Bacteroides* was significantly negatively correlated with the content of various SCFAs, among which it was significantly negatively correlated with i-butyric acid ($r = -0.981$, $p < 0.05$), i-valeric acid ($r = -0.999$, $p < 0.01$), n-valeric acid ($r = -0.993$, $p < 0.01$), and caproic acid ($r = -0.962$, $p < 0.05$). On the contrary, the relative abundance of *Alistipes* was significantly positively correlated with propionic acid content ($r = 0.968$, $p < 0.05$).

## 4 | Discussion

IBD is a group of chronic, relapsing inflammatory disorders of the gut that seriously threaten human health and currently have many treatment limitations, making clinical management challenging (Vancamelbeke et al. 2017; Bao et al. 2023; Yuan et al. 2023). Searching for safe and effective natural treatments could offer a solution. Based on previous in vivo and in vitro studies, we aimed to explore further the mechanism by which AP1 effectively inhibits the DSS-induced UC process in mice.

According to the previous hypothesis, we started this study by focusing first on the cell from the pathological damage of the mucosal barrier. Initially, we investigated the effects of AP1 on intestinal mucosal epithelial cells. Our results showed a dose-dependent increase in goblet cell numbers following AP1 treatment, suggesting its potential restorative effects on goblet cell populations. In addition, dynamic body weight changes, a well-established phenotypic marker of DSS-induced colitis, were comprehensively monitored in our previously published study (Peng, Zhu, et al. 2024). These data demonstrated that AP1 treatment significantly mitigated DSS-induced weight loss in a dose-dependent manner, consistent with the observed improvements in DAI scores and histopathology. Ma et al. have previously

shown that modified Gegen Qinlian plays a role in the restoration of goblet cell function for the repair of the intestinal mucus barrier in mice with DSS-induced chronic colitis (Ma et al. 2023). Numerous studies have focused on barrier-related genes (e.g., MUC1, MUC4, and MUC22) and components (e.g., the mucosal layer and regulatory proteins) that may induce or maintain chronic intestinal inflammation in UC (Vancamelbeke et al. 2017; Xu et al. 2019; Xiao et al. 2022). Dysregulation of epithelial barrier genes, especially mucoid layer genes, has been found in inflamed areas of UC patients, with MUC1 and MUC4 often dysregulated even in inactive disease (Vancamelbeke et al. 2017). The mucus layer protects the epithelium, and goblet cell dysfunction in the mucosal epithelium of mice leads to issues such as increased bacterial adhesion and susceptibility to colitis (Kim and Ho 2010; Yao et al. 2021; Brockhausen et al. 2024). Continued bacterial stimulation can exacerbate goblet cell dysfunction and contribute to colitis (Ma et al. 2023). Based on previous findings that AP1 enhances intestinal mucosal protection and may prevent pathogen invasion by improving barrier function (Peng, Zhu, et al. 2024), we hypothesized that AP1 alleviates colitis symptoms in mice by increasing goblet cells and restoring intestinal barrier function (J. Yang, Xiao, et al. 2024). Specific barrier-related SNPs are enriched in CD and UC-related genes, with a SNP in MUC21 identified as associated with UC (Achkar et al. 2012; Vancamelbeke et al. 2017). This suggested that a subset of UC patients may have a genetic predisposition to barrier defects. Phosphatidylcholine is currently one of the most promising therapeutic targets for UC, and it is released slowly through the major phospholipids in the colonic mucus layer to reinforce the mucus layer (Karner et al. 2014; Vancamelbeke et al. 2017). This treatment provides strong evidence supporting the restoration of the mucosal barrier as a means to improve UC status. These findings align with our results, where AP1 restored the mucosal barrier and repaired intestinal tissue.

Inflammatory and immune system disorders are common causes of chronic IBD (Kwon et al. 2024). Goblet cells also play a critical role in immune regulation in the gut (Tonetti et al. 2024). Their reduction suggests impaired intestinal barrier function and local immune dysregulation (Cornick et al. 2015). The spleen, an important immune organ, reflects the level of immune activation through changes in its weight (Tarantino et al. 2013; Lewis et al. 2019; El-Naseery et al. 2020; Kawashima et al. 2022). When intestinal immune function was disrupted, a systemic immune response was triggered (S. Yang and Yu 2021). We, therefore, hypothesized that the reduction in goblet cells may not only have resulted from local inflammatory responses in the colon but may also have triggered systemic immune responses. In this study, we tested changes in spleen weight. AP1 effectively attenuated the systemic immune response and exhibited an immunoregulatory effect like that of 5-ASA. This is consistent with previous studies (X. Chen et al. 2019; Kawashima et al. 2022; Y. Yang et al. 2023). In this study, we found that AP1 significantly reduced the levels of proinflammatory cytokines TNF-$\alpha$, IL-1$\beta$, and IL-18 in colonic tissue in a dose-dependent manner. These findings complement previous studies and confirm that AP1 effectively inhibits key proinflammatory cytokines at both mRNA and protein levels. Some studies have reported that natural compounds (COP, ABP, and columbianadin) alleviate UC through complementary mechanisms targeting both inflammatory and oxidative pathways (Cury et al. 2024; C. Li et al. 2024; Y. Zhang, Cao, et al. 2025). These
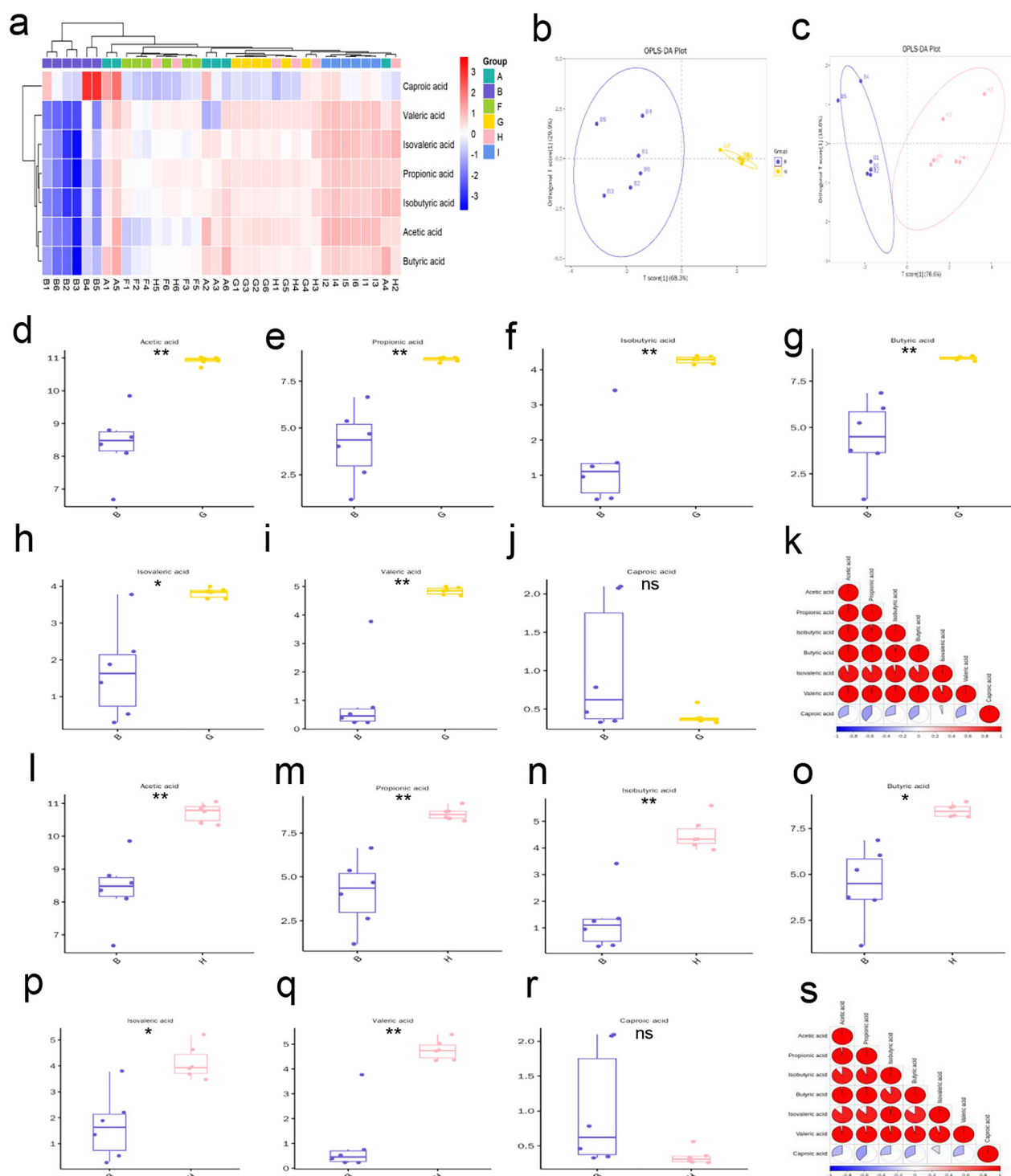
**FIGURE 6** | AP1 treatment increased the production of microbial metabolite SCFAs. (a) Cluster heatmap analysis. (b) OPLS-DA analyzed between DSS group and AP1–M group. (c) OPLS-DA analyzed between DSS group and AP1–H group. (d) Acetic acid. (e) Propionic acid. (f) i-Butyric acid. (g) Butyric acid. (h) i-Valeric acid. (i) Valeric acid. (j) Caproic acid. (k) Correlation heatmap relatively contents contrasted DSS group to AP1–M group. (l) Acetic acid. (m) Propionic acid. (n) i-Butyric acid. (o) Butyric acid. (p) i-Valeric acid. (q) Valeric acid. (r) Caproic acid. (s) Correlation heatmap relatively contents contrasted DSS group to AP1–H group. *$p < 0.05$, **$p < 0.01$, ***$p < 0.001$.

findings were consistent with ours; we thus trusted that AP1 has antioxidant effects and can alleviate colonic tissue damage caused by oxidative stress. In addition, our previous work (Peng, Li, et al. 2024; Peng, Zhu, et al. 2024) demonstrated at the protein level that AP1 significantly reduced NF-$\kappa$B p65 and COX-2 expression

in DSS-induced UC mice, thereby confirming its direct action on the NF-$\kappa$B pathway. While these assays were not repeated here to avoid redundancy, the current study complements those findings by expanding the mechanistic framework to gut microbiota modulation and SCFA restoration. Together, these results
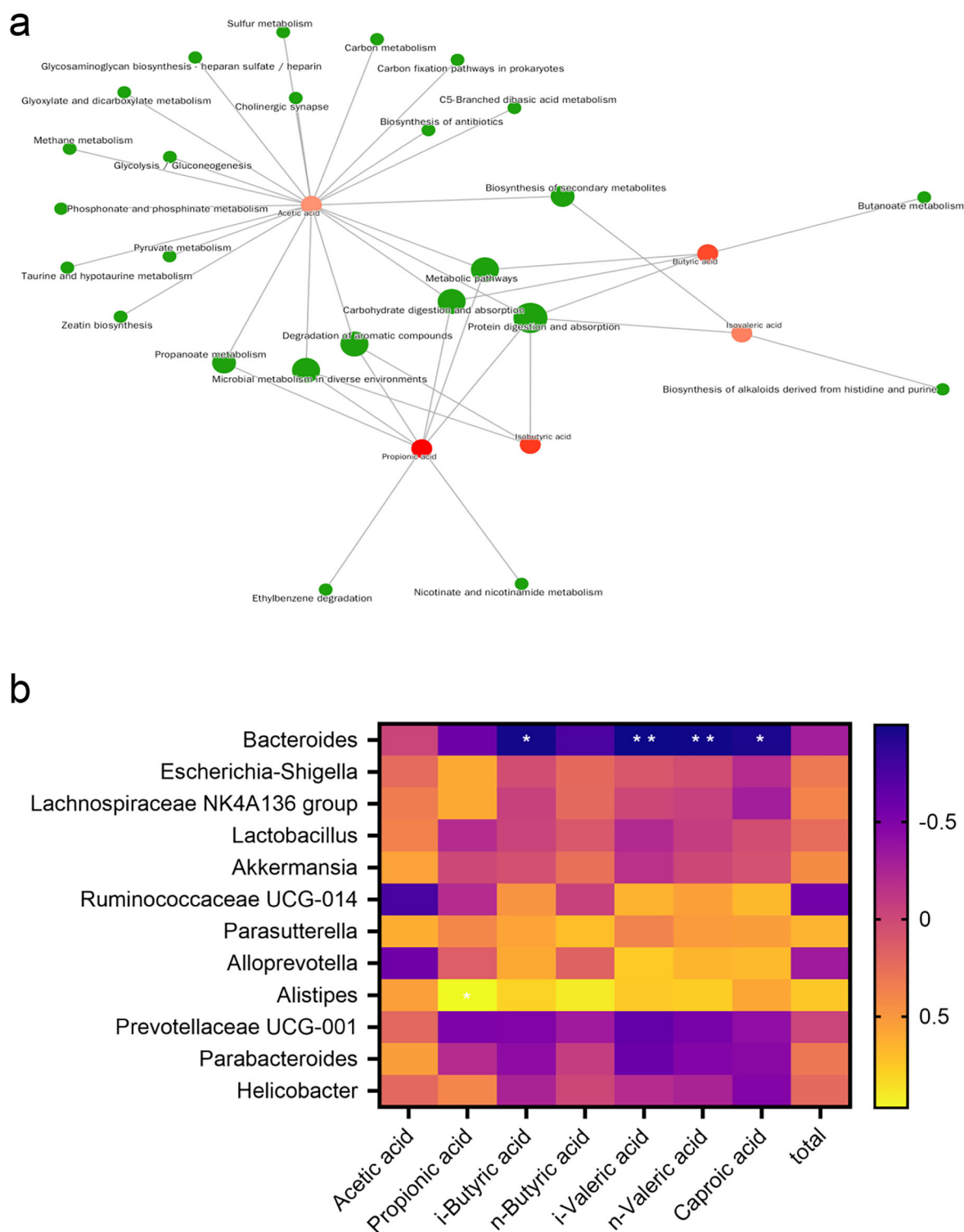
**FIGURE 7** | KEGG analysis of metabolites and correlation analysis of SCFAs and gut microbes. (a) KEGG metabolite molecular network map. (b) Correlation analysis of SCFAs and gut microbes at the genus-level. Red and blue blocks represent positive and negative correlations, respectively. Statistical significance is indicated by $*p < 0.05$, $**p < 0.01$.

provide converging evidence that AP1 exerts its therapeutic effects through both direct anti-inflammatory signaling (via NF-$\kappa$B inhibition) and indirect regulation of the gut–immune–microbiota axis. We speculated that AP1's antioxidant function reduces MDA levels and increases CAT activity by activating antioxidant enzymes or inhibiting oxidative stress pathways, such as the

Nrf2 pathway or the NADPH oxidase pathway. There may be a synergistic effect between the antioxidant and anti-inflammatory effects, promoting recovery from colitis.

A balanced gut microbiota is essential for maintaining immune homeostasis and preserving intestinal barrier function. DSS-

induced disruption of the mucosal layer increases intestinal permeability, allowing bacterial translocation and compromising colonic epithelial integrity. Under these conditions induced by DSS, along with gut microbiota disruption, microbial components enter the mucosa, playing a critical role in the development of DSS-induced colitis (Johansson et al. 2010; Hernández-Chirlaque et al. 2016; C. Yang and Merlin 2024). The gut microbiota creates a chronic inflammatory microenvironment, leading to DNA damage, chromosome mutations, and altered production of specific metabolites critical for colon cancer development (Xia et al. 2024). Many scientists have focused on bacteriotherapy to restore the homeostasis of the gut microbiota (P. Guo et al. 2024). Previous studies have investigated dysbiosis associated with IBD, focusing on structural changes related to pathogenesis, metabolic dysfunction, disease prognosis, and predictors of therapeutic response (Zuo and Ng 2018; Tsai et al. 2025). Consistent with some studies (Man et al. 2011), we identified the DSS-induced disruption of gut microbiota homeostasis in colitis mice. This variation in microbiota composition is closely linked to the development of intestinal inflammation. In addition, changes in the abundance of *Firmicutes* and *Bacteroidetes* species were often associated with different diseases (Letchumanan et al. 2022), with a characteristic decrease in Bacteroidetes and an increase in Firmicutes under pathological conditions (Komodromou et al. 2024; Min et al. 2024; Paziewska et al. 2024). AP1 treatment most markedly altered the relative abundances of Bacteroidetes and Firmicutes in the gut microbiota of DSS-induced UC mice. Furthermore, the increase in Firmicutes was dose-dependent, which may indicate that AP1 preferentially promotes Firmicutes-associated taxa that are commonly linked to SCFA production. Compared with other natural polysaccharides, AP1 showed a more consistent and dose-dependent modulation of gut microbiota, potentially leading to greater restoration of SCFA-producing bacteria and more robust anti-inflammatory effects (Zheng et al. 2025). Regarding microbiota changes specifically at the family and genus level, we observed that AP1 increased the relative abundance of beneficial bacteria (such as *Lachnospiraceae*, *Prevotellaceae*, and *Akkermansiaceae*) while decreasing harmful bacteria, correcting DSS-induced gut microbiota perturbation. The beneficial bacteria *Lachnospiraceae* produce SCFAs, which have anti-inflammatory properties (Cao et al. 2024; F. Yang, Su, et al. 2024). Conversely, *Bacteroidaceae* and *Tannerellaceae* decreased with AP1. *Bacteroidaceae* includes *Bacteroides*, which can be beneficial but might be pathogenic in specific contexts (Shin et al. 2024). In our study, *Bacteroidaceae*, *Desulfovibrionaceae*, and *Tannerellaceae* showed dose-dependent recovery of abundance after AP1 treatment, and the abundance of bacteria in the AP1–H group was closer to the control group compared to the 5-ASA group. So, we can suppose their changes here might indicate a shift away from dysbiosis. These findings suggest that AP1 may be a potential treatment for regulating gut microbiota disorders, with possibly fewer side effects than current treatments. Further analysis of microbial diversity and community structure revealed that AP1 treatment significantly increased the abundance of dominant bacterial groups and improved overall gut microbiota diversity. NMDS and PCoA analyses demonstrated that the bacterial composition in AP1-treated mice was closely aligned with that of the control group. Moreover, LEfSe analysis identified significant differences in bacterial taxa among the experimental groups. The dominant bacterial groups after AP1 treatment were primarily gut probiotics. Sanchis-Artero et al. (2021) suggested

that IBD reduces bacterial diversity and richness, possibly due to the loss of normal anaerobic bacteria, such as *Bacteroides* species. *Bacteroidaceae* and *Desulfovibrionaceae* were associated with intestinal inflammation (Osaka et al. 2017; C.-X. Li et al. 2023; X. Li, Sun, et al. 2025), while *Tannerellaceae* belonged to the phylum *Bacteroidetes* (Jean et al. 2022). The metabolic activities of these obligate anaerobes were closely linked to oxygen availability within the intestinal microenvironment (J. Chen and Vitetta 2020). Furthermore, it has been documented that the oxygen tension at the surface of the intestinal mucosa can exhibit significant fluctuations, particularly during periods of inflammation (Glover et al. 2013). Therefore, we speculated that the dose-dependent regulation of microbiota abundance by AP1 may be mediated through mechanisms involving improved local oxygen tension or modulation of host–microbiota interactions. In addition, we found that AP1 has prebiotic properties for UC mice, promoting beneficial bacterial growth or exhibiting anti-inflammatory properties that enhance the environment for beneficial bacteria, consistent with our previous findings on AP1 interventions in healthy humans (Peng et al. 2023; Peng, Li, et al. 2024). Many studies on polysaccharide function support this idea (Alonso-Allende et al. 2024; Kang and Chang 2024; X. Liu, Zhang, et al. 2024; Pan et al. 2025). Thus, AP1 positively regulates the gut microbiota.

SCFAs generated through bacterial fermentation of dietary fiber play a pivotal role in maintaining the epithelial barrier integrity and modulating immune responses (Silva et al. 2020; Deng et al. 2021; Ikeda and Matsuda 2023; Du et al. 2024; Mann et al. 2024). Therefore, SCFAs are a critical link between the gut microbiota and intestinal health in the host. Our findings show that DSS-induced colitis significantly impaired SCFA production. The reduction in SCFA levels indicates substantial impairment of microbial metabolic activity under inflammatory conditions. AP1 administration effectively reversed this depletion in a dose-dependent manner, underscoring its role in restoring microbial metabolic function. Compared with other natural polysaccharides, AP1 exhibited a more pronounced effect on restoring SCFA levels, particularly butyrate, highlighting its potential superiority in modulating gut microbial metabolism. These metabolic alterations corresponded with the observed shifts in gut microbial composition following AP1 treatment. The restoration of SCFAs, especially butyrate, likely resulted from AP1-driven enrichment of *Firmicutes*, known for their SCFA-producing species. Our findings support previous evidence of butyrate's anti-inflammatory properties (Deng et al. 2021; Ikeda and Matsuda 2023), showing that AP1 elevated butyrate levels and normalized BCFAs, such as i-butyric and i-valeric acids, at the AP1–H group. This finding was consistent with other studies suggesting that the metabolic effects of i-butyric acid are increasingly recognized for their anti-inflammatory properties and for supporting intestinal barrier integrity. However, potential side effects or limitations of AP1 supplementation, particularly at high doses, remain to be evaluated, including possible gastrointestinal disturbances or metabolic imbalances. In animal models of UC, both i-butyric and i-valeric acids improved symptoms and reduced inflammation (W.-W. Zhang et al. 2024; Xin et al. 2025). Furthermore, AP1–M has emerged as the optimal dose for restoring major SCFAs (acetic, propionic, and n-butyric acids), achieving concentrations comparable to the control group and similar to those in the AP1–H group. Some studies support our

research results, concluding that acetic acid, propionic acid, and n-butyric acid exhibit notable anti-inflammatory properties and influence immune responses (Tao et al. 2025; Wang et al. 2025; S. Zhang, Wang, et al. 2025). Conversely, AP1–L exhibited minimal efficacy in regulating n-butyric acid or BCFAs. Mechanistically, AP1 likely alleviates colitis through dual actions. Restoration of SCFAs biosynthesis enhances barrier function and mitigates mucosal inflammation. The microbiota should be restructured by promoting *Firmicutes*/SCFA producers and inhibiting *Bacteroidetes*/substrate competitors. Our findings are consistent with previous research (H. Li et al. 2022).

The present study elucidated the role of AP1 in protecting against DSS-induced UC in mice by restoring the function of the mucosal barrier, attenuating the local inflammatory reactions in the colon, and balancing the gut microbiota and SCFAs production. Although AP1 was an effective plant-derived polysaccharide and showed good therapeutic effects in mice, potential safety concerns at high doses, including gastrointestinal discomfort or metabolic alterations, warrant careful evaluation before human application. Further investigation is required into its safety and optimal dosage before human application. This should include examining potential side effects and adverse effects, systematically assess dose-dependent toxicity, and determining safe upper limits through preclinical studies. To provide a solid foundation for the clinical application of AP1, further in vivo studies and human clinical trials are needed to investigate its mechanism of action, as well as to confirm its efficacy and safety profile in diverse patient populations. Future research should also explore the potential application of AP1 in new clinical trials, including its long-term efficacy, optimal dosing regimens, and potential combinatory use with existing therapies for UC.

## 5 | Conclusion

In conclusion, this study demonstrated the beneficial effects of AP1 in treating DSS-induced UC in mice. We observed that AP1 significantly regulated intestinal barrier function in UC mice, attenuated DSS-induced mucosal cell apoptosis, and reduced inflammation and oxidative stress. In addition, AP1 influenced gut microbiota diversity in UC mice, which may provide further insight into UC pathogenesis and the immunomodulatory effects of AP1. Therefore, we conclude that AP1 has the potential to be an effective treatment for UC, providing a solid theoretical basis for its use in treating human IBD.

**Author Contributions**

**Yanqi Peng**: conceptualization, formal analysis, validation, software, and writing – original draft. **Ji Wu**: investigation, data curation, visualization, validation, writing – review. **Ronghua Fan** and **Mingyue Ma**: project administration, investigation, methodology. **Xixin Wang**: visualization. **Yuzhen Pi**: investigation, data curation, validation. **Xiqing Yue**: funding acquisition, supervision, resources, project administration. **Yanyu Peng**: review and editing, project administration, data curation, funding acquisition. All authors agree to account for all aspects of the work, ensuring integrity and accuracy.

**Conflicts of Interest**

The authors declare no conflicts of interest.

**Data Availability Statement**

Data will be made available on request.

## References

Achkar, J.-P., L. Klei, P. I. W. de Bakker, et al. 2012. "Amino Acid Position 11 of HLA-DRβ1 Is a Major Determinant of Chromosome 6p Association With Ulcerative Colitis." *Genes and Immunity* 13: 245–252. https://doi.org/10.1038/gene.2011.79.

Alonso-Allende, J., F. I. Milagro, and P. Aranaz. 2024. "Health Effects and Mechanisms of Inulin Action in Human Metabolism." *Nutrients* 16: 2935. https://doi.org/10.3390/nu16172935.

Bao, M., K. Wang, J. Li, et al. 2023. "ROS Scavenging and Inflammation-Directed Polydopamine Nanoparticles Regulate Gut Immunity and Flora Therapy in Inflammatory Bowel Disease." *Acta Biomaterialia* 161: 250–264. https://doi.org/10.1016/j.actbio.2023.02.026.

Beaugerie, L., and S. H. Itzkowitz. 2015. "Cancers Complicating Inflammatory Bowel Disease." *New England Journal of Medicine* 372: 1441–1452. https://doi.org/10.1056/NEJMra1403718.

Brockhausen, I., D. Falconer, and S. Sara. 2024. "Relationships Between Bacteria and the Mucus Layer." *Carbohydrate Research* 546: 109309. https://doi.org/10.1016/j.carres.2024.109309.

Cao, J., L. Qin, L. Zhang, et al. 2024. "Protective Effect of Cellulose and Soluble Dietary Fiber From *Saccharina japonica* By-Products on Regulating Inflammatory Responses, Gut Microbiota, and SCFAs Production in Colitis Mice." *International Journal of Biological Macromolecules* 267: 131214. https://doi.org/10.1016/j.ijbiomac.2024.131214.

Chen, J., and L. Vitetta. 2020. "The Role of Butyrate in Attenuating Pathobiont-Induced Hyperinflammation." *Immune Network* 20: e15. https://doi.org/10.4110/in.2020.20.e15.

Chen, X., Z. Sheng, S. Qiu, et al. 2019. "Purification, Characterization and In Vitro and In Vivo Immune Enhancement of Polysaccharides From Mulberry Leaves." *PLoS One* 14: e0208611. https://doi.org/10.1371/journal.pone.0208611.

Chen, Y.-E., S.-J. Xu, Y.-Y. Lu, et al. 2021. "Asperuloside Suppressing Oxidative Stress and Inflammation in DSS-Induced Chronic Colitis and RAW 264.7 Macrophages via Nrf2/HO-1 and NF-κB Pathways." *Chemico-Biological Interactions* 344: 109512. https://doi.org/10.1016/j.cbi.2021.109512.

Cornick, S., A. Tawiah, and K. Chadee. 2015. "Roles and Regulation of the Mucus Barrier in the Gut." *Tissue Barriers* 3: e982426. https://doi.org/10.4161/21688370.2014.982426.

Cury, B. J., D. T. Jerônimo, L. M. Da Silva, et al. 2024. "Hydroalcoholic Extract of *Araucaria* sp. Brown Propolis Alleviates Ulcerative Colitis Induced by TNBS in Rats by Reducing Inflammatory Cell Infiltration and Oxidative Damage." *Journal of Pharmacy and Pharmacology* 76: 1379–1392. https://doi.org/10.1093/jpp/rgae083.

Deng, M., X. Wu, X. Duan, et al. 2021. "*Lactobacillus paracasei* L9 Improves Colitis by Expanding Butyrate-Producing Bacteria That Inhibit the IL-6/STAT3 Signaling Pathway." *Food & Function* 12: 10700–10713. https://doi.org/10.1039/d1fo02077c.

Du, Y., C. He, Y. An, et al. 2024. "The Role of Short Chain Fatty Acids in Inflammation and Body Health." *International Journal of Molecular Sciences* 25: 7379. https://doi.org/10.3390/ijms25137379.

El-Naseery, N. I., H. S. E. Mousa, A. E. Noreldin, A. H. El-Far, and Y. H. A. Elewa. 2020. "Aging-Associated Immunosenescence via Alterations in Splenic Immune Cell Populations in Rat." *Life Sciences* 241: 117168. https://doi.org/10.1016/j.lfs.2019.117168.

Fang, J., H. Wang, Y. Zhou, H. Zhang, H. Zhou, and X. Zhang. 2021. "Slimy Partners: The Mucus Barrier and Gut Microbiome in Ulcerative Colitis." *Experimental & Molecular Medicine* 53: 772–787. https://doi.org/10.1038/s12276-021-00617-8.

Gao, H., S. Zheng, X. Yuan, J. Xie, and L. Xu. 2023. "Causal Association Between Inflammatory Bowel Disease and 32 Site-Specific Extracolonic Cancers: A Mendelian Randomization Study." *BMC Medicine* 21: 389. https://doi.org/10.1186/s12916-023-03096-y.

Glover, L. E., B. E. Bowers, B. Saeedi, et al. 2013. "Control of Creatine Metabolism by HIF Is an Endogenous Mechanism of Barrier Regulation in Colitis." *PNAS* 110: 19820–19825. https://doi.org/10.1073/pnas.1302840110.

Graham, D. B., and R. J. Xavier. 2020. "Pathway Paradigms Revealed From the Genetics of Inflammatory Bowel Disease." *Nature* 578: 527–539. https://doi.org/10.1038/s41586-020-2025-2.

Guo, P., W. Wang, Q. Xiang, et al. 2024. "Engineered Probiotic Ameliorates Ulcerative Colitis by Restoring Gut Microbiota and Redox Homeostasis." *Cell Host & Microbe* 32: 1502–1518.e9. https://doi.org/10.1016/j.chom.2024.07.028.

Guo, X. Y., X. J. Liu, and J. Y. Hao. 2020. "Gut Microbiota in Ulcerative Colitis: Insights on Pathogenesis and Treatment." *Journal of Digestive Diseases* 21: 147–159. https://doi.org/10.1111/1751-2980.12849.

Han, X., J. Guo, Y. You, et al. 2018. "A Fast and Accurate Way to Determine Short Chain Fatty Acids in Mouse Feces Based on GC-MS." *Journal of Chromatography B: Analytical Technologies in the Biomedical and Life Sciences* 1099: 73–82. https://doi.org/10.1016/j.jchromb.2018.09.013.

Hernández-Chirlaque, C., C. J. Aranda, B. Ocón, et al. 2016. "Germ-Free and Antibiotic-Treated Mice Are Highly Susceptible to Epithelial Injury in DSS Colitis." *Journal of Crohn's and Colitis* 10: 1324–1335. https://doi.org/10.1093/ecco-jcc/jjw096.

Hsu, Y.-L., C.-C. Chen, Y.-T. Lin, et al. 2019. "Evaluation and Optimization of Sample Handling Methods for Quantification of Short-Chain Fatty Acids in Human Fecal Samples by GC-MS." *Journal of Proteome Research* 18: 1948–1957. https://doi.org/10.1021/acs.jproteome.8b00536.

Ikeda, Y., and S. Matsuda. 2023. "Gut Protective Effect From D-Methionine or Butyric Acid Against DSS and Carrageenan-Induced Ulcerative Colitis." *Molecules* 28: 4392. https://doi.org/10.3390/molecules28114392.

Jean, S., M. J. Wallace, G. Dantas, and C.-A. D. Burnham. 2022. "Time for Some Group Therapy: Update on Identification, Antimicrobial Resistance, Taxonomy, and Clinical Significance of the *Bacteroides fragilis* Group." *Journal of Clinical Microbiology* 60: e0236120. https://doi.org/10.1128/jcm.02361-20.

Johansson, M. E. V., J. K. Gustafsson, K. E. Sjöberg, et al. 2010. "Bacteria Penetrate the Inner Mucus Layer Before Inflammation in the Dextran Sulfate Colitis Model." *PLoS One* 5: e12238. https://doi.org/10.1371/journal.pone.0012238.

Kang, Y. R., and Y. H. Chang. 2024. "Structural Characterization and Prebiotic Activity of Rhamnogalacturonan-I Rich Pumpkin Pectic Polysaccharide Extracted by Alkaline Solution." *International Journal of Biological Macromolecules* 270: 132311. https://doi.org/10.1016/j.ijbiomac.2024.132311.

Karner, M., A. Kocjan, J. Stein, et al. 2014. "First Multicenter Study of Modified Release Phosphatidylcholine "LT-02" in Ulcerative Colitis: A Randomized, Placebo-Controlled Trial in Mesalazine-Refractory Courses." *American Journal of Gastroenterology* 109: 1041–1051. https://doi.org/10.1038/ajg.2014.104.

Kaviani, E., M. Rahmani, A. Kaeidi, et al. 2017. "Protective Effect of Atorvastatin on D-Galactose-Induced Aging Model in Mice." *Behavioural Brain Research* 334: 55–60. https://doi.org/10.1016/j.bbr.2017.07.029.

Kawashima, K., M. Onizawa, T. Fujiwara, et al. 2022. "Evaluation of the Relationship Between the Spleen Volume and the Disease Activity in Ulcerative Colitis and Crohn Disease." *Medicine* 101: e28515. https://doi.org/10.1097/MD.0000000000028515.

Kim, Y. S., and S. B. Ho. 2010. "Intestinal Goblet Cells and Mucins in Health and Disease: Recent Insights and Progress." *Current Gastroenterology Reports* 12: 319–330. https://doi.org/10.1007/s11894-010-0131-2.

Komodromou, I., E. Andreou, A. Vlahoyiannis, et al. 2024. "Exploring the Dynamic Relationship Between the Gut Microbiome and Body Composition Across the Human Lifespan: A Systematic Review." *Nutrients* 16: 660. https://doi.org/10.3390/nu16050660.

Kwon, S. J., M. S. Khan, and S. G. Kim. 2024. "Intestinal Inflammation and Regeneration-Interdigitating Processes Controlled by Dietary Lipids in Inflammatory Bowel Disease." *International Journal of Molecular Sciences* 25: 1311. https://doi.org/10.3390/ijms25021311.

Letchumanan, G., N. Abdullah, M. Marlini, et al. 2022. "Gut Microbiota Composition in Prediabetes and Newly Diagnosed Type 2 Diabetes: A Systematic Review of Observational Studies." *Frontiers in Cellular and Infection Microbiology* 12: 943427. https://doi.org/10.3389/fcimb.2022.943427.

Lewis, S. M., A. Williams, and S. C. Eisenbarth. 2019. "Structure and Function of the Immune System in the Spleen." *Science Immunology* 4: eaau6085. https://doi.org/10.1126/sciimmunol.aau6085.

Li, C., L. Deng, M. Pu, X. Ye, and Q. Lu. 2024. "Coptisine Alleviates Colitis Through Modulating Gut Microbiota and Inhibiting TXNIP/NLRP3 Inflammasome." *Journal of Ethnopharmacology* 335: 118680. https://doi.org/10.1016/j.jep.2024.118680.

Li, C.-X., Y.-M. Wang, W.-J. Zhang, et al. 2023. "IL-10-Dependent Effect of Chinese Medicine *Abelmoschus manihot* on Alleviating Intestinal Inflammation and Modulating Gut Microbiota." *American Journal of Chinese Medicine* 51: 1527–1546. https://doi.org/10.1142/S0192415x23500696.

Li, H., W. Cao, J. Xie, et al. 2022. "α-D-1,6-Glucan From *Castanea mollissima* Blume Alleviates Dextran Sulfate Sodium-Induced Colitis In Vivo." *Carbohydrate Polymers* 289: 119410. https://doi.org/10.1016/j.carbpol.2022.119410.

Li, H., L. Fan, S. Yang, et al. 2025. "*Lactobacillus acidophilus* 6074 Fermented Jujube Juice Ameliorated DSS-Induced Colitis via Repairing Intestinal Barrier, Modulating Inflammatory Factors, and Gut Microbiota." *Molecular Nutrition & Food Research* 69: e202400568. https://doi.org/10.1002/mnfr.202400568.

Li, X., B. Sun, Y. Qin, F. Yue, and X. Lü. 2025. "Amelioration of Obesity-Related Disorders in High-Fat Diet-Fed C57BL/6 Mice Following Fecal Microbiota Transplantation From DL-Norvaline-Dosed Mice." *Molecular Nutrition & Food Research* 69: e202400577. https://doi.org/10.1002/mnfr.202400577.

Li, Z., S. Zhu, Q. Liu, et al. 2020. "Polystyrene Microplastics Cause Cardiac Fibrosis by Activating Wnt/β-Catenin Signaling Pathway and Promoting Cardiomyocyte Apoptosis in Rats." *Environmental Pollution* 265: 115025. https://doi.org/10.1016/j.envpol.2020.115025.

Liu, M., G. Guan, Y. Wang, X. Lu, X. Duan, and X. Xu. 2024. "*p*-Hydroxy Benzaldehyde, a Phenolic Compound From *Nostoc commune*, Ameliorates DSS-Induced Colitis Against Oxidative Stress via the Nrf2/HO-1/NQO-1/NF-κB/AP-1 Pathway." *Phytomedicine* 133: 155941. https://doi.org/10.1016/j.phymed.2024.155941.

Liu, X., M. Zhang, S. Chen, et al. 2024. "*Grifola frondosa* Polysaccharide's Therapeutic Potential in Oxazolone-Induced Ulcerative Colitis." *Carbohydrate Polymers* 344: 122517. https://doi.org/10.1016/j.carbpol.2024.122517.

Ma, J., J. Zhang, Y. Wang, et al. 2023. "Modified Gegen Qinlian Decoction Ameliorates DSS-Induced Chronic Colitis in Mice by Restoring the

Intestinal Mucus Barrier and Inhibiting the Activation of $\gamma\delta17$ Cells." *Phytomedicine* 111: 154660. https://doi.org/10.1016/j.phymed.2023.154660.

Man, S. M., N. O. Kaakoush, and H. M. Mitchell. 2011. "The Role of Bacteria and Pattern-Recognition Receptors in Crohn's Disease." *Nature Reviews Gastroenterology & Hepatology* 8: 152–168. https://doi.org/10.1038/nrgastro.2011.3.

Mann, E. R., Y. K. Lam, and H. H. Uhlig. 2024. "Short-Chain Fatty Acids: Linking Diet, the Microbiome and Immunity." *Nature Reviews Immunology* 24: 577–595. https://doi.org/10.1038/s41577-024-01014-8.

Min, L., A. Ablitip, R. Wang, T. Luciana, M. Wei, and X. Ma. 2024. "Effects of Exercise on Gut Microbiota of Adults: A Systematic Review and Meta-Analysis." *Nutrients* 16: 1070. https://doi.org/10.3390/nu16071070.

Osaka, T., E. Moriyama, S. Arai, et al. 2017. "Meta-Analysis of Fecal Microbiota and Metabolites in Experimental Colitic Mice During the Inflammatory and Healing Phases." *Nutrients* 9: 1329. https://doi.org/10.3390/nu9121329.

Pan, L., L. Wang, Z. Zeng, Z. Zhang, B. Zheng, and Y. Zhang. 2025. "Chemical Structure and Prebiotic Activity of a *Dictyophora indusiata* Polysaccharide Fraction." *Food Chemistry* 463: 141086. https://doi.org/10.1016/j.foodchem.2024.141086.

Paone, P., and P. D. Cani. 2020. "Mucus Barrier, Mucins and Gut Microbiota: The Expected Slimy Partners?" *Gut* 69: 2232–2243. https://doi.org/10.1136/gutjnl-2020-322260.

Paziewska, M., M. Szelest, M. Kiełbus, et al. 2024. "Increased Abundance of Firmicutes and Depletion of Bacteroidota Predicts Poor Outcome in Chronic Lymphocytic Leukemia." *Oncology Letters* 28: 552. https://doi.org/10.3892/ol.2024.14685.

Peng, Y., Y. Li, Y. Pi, and X. Yue. 2024. "Effects of Almond (*Armeniaca sibirica* L. Lam) Polysaccharides on Gut Microbiota and Anti-Inflammatory Effects on LPS-Induced RAW264.7 Cells." *International Journal of Biological Macromolecules* 263, no. Pt 1: 130098. https://doi.org/10.1016/j.ijbiomac.2024.130098.

Peng, Y., Z. Zhang, W. Chen, S. Zhao, Y. Pi, and X. Yue. 2023. "Structural Characterization, $\alpha$-Glucosidase Inhibitory Activity and Antioxidant Activity of Neutral Polysaccharide From Apricot (*Armeniaca sibirica* L. Lam) Kernels." *International Journal of Biological Macromolecules* 238: 124109. https://doi.org/10.1016/j.ijbiomac.2023.124109.

Peng, Y., J. Zhu, Y. Li, X. Yue, and Y. Peng. 2024. "Almond Polysaccharides Inhibit DSS-Induced Inflammatory Response in Ulcerative Colitis Mice Through NF-$\kappa$B Pathway." *International Journal of Biological Macromolecules* 281, no. Pt 1: 136206. https://doi.org/10.1016/j.ijbiomac.2024.136206.

Prame Kumar, K., J. D. Ooi, and R. Goldberg. 2023. "The Interplay Between the Microbiota, Diet and T Regulatory Cells in the Preservation of the Gut Barrier in Inflammatory Bowel Disease." *Frontiers in Microbiology* 14: 1291724. https://doi.org/10.3389/fmicb.2023.1291724.

Sanchis-Artero, L., J. F. Martínez-Blanch, S. Manresa-Vera, et al. 2021. "Evaluation of Changes in Intestinal Microbiota in Crohn's Disease Patients After Anti-TNF-$\alpha$ Treatment." *Scientific Reports* 11: 10016. https://doi.org/10.1038/s41598-021-88823-2.

Shi, D.-C., P.-Y. Wang, L. Xu, et al. 2025. "Potential of *Dendrobium officinale* Oligosaccharides to Alleviate Chronic Colitis by Modulating Inflammation and Gut Microbiota." *Food & Medicine Homology* 2, no. 3: 9420077. https://doi.org/10.26599/FMH.2025.9420077.

Shin, J. H., G. Tillotson, T. N. Mackenzie, C. A. Warren, H. M. Wexler, and E. J. C. Goldstein. 2024. "Bacteroides and Related Species: The Keystone Taxa of the Human Gut Microbiota." *Anaerobe* 85: 102819. https://doi.org/10.1016/j.anaerobe.2024.102819.

Silva, Y. P., A. Bernardi, and R. L. Frozza. 2020. "The Role of Short-Chain Fatty Acids from Gut Microbiota in Gut-Brain Communication." *Frontiers in Endocrinology* 11: 25. https://doi.org/10.3389/fendo.2020.00025.

Tao, M., Y. Xie, X. Fan, et al. 2025. "Neutral Polysaccharide From *Dendrobium officinale* Alleviates Acute Alcohol-Induced Liver Injury via the Gut Microbiota-Short Chain Fatty Acids-Liver Axis." *International Journal of Biological Macromolecules* 317: 144719. https://doi.org/10.1016/j.ijbiomac.2025.144719.

Tarantino, G., A. Scalera, and Y. Xie. 2013. "Liver-Spleen Axis: Intersection Between Immunity, Infections and Metabolism." *World Journal of Gastroenterology* 19: 3534–3542. https://doi.org/10.3748/wjg.v19.i23.3534.

Tocmo, R., B. Le, A. Heun, J. P. Van Pijkeren, K. Parkin, and J. J. Johnson. 2021. "Prenylated Xanthones From Mangosteen (*Garcinia mangostana*) Activate the AhR and Nrf2 Pathways and Protect Intestinal Barrier Integrity in HT-29 Cells." *Free Radical Biology and Medicine* 163: 102–115. https://doi.org/10.1016/j.freeradbiomed.2020.11.018.

Tonetti, F. R., A. Eguileor, and C. Llorente. 2024. "Goblet Cells: Guardians of Gut Immunity and Their Role in Gastrointestinal Diseases." *Egastroenterology* 2: e100098. https://doi.org/10.1136/egastro-2024-100098.

Tsai, Y.-C., W.-C. Tai, C.-M. Liang, et al. 2025. "Alternations of the Gut Microbiota and the Firmicutes/Bacteroidetes Ratio After Biologic Treatment in Inflammatory Bowel Disease." *Journal of Microbiology, Immunology and Infection* 58: 62–69. https://doi.org/10.1016/j.jmii.2024.09.006.

Vancamelbeke, M., T. Vanuytsel, R. Farré, et al. 2017. "Genetic and Transcriptomic Bases of Intestinal Epithelial Barrier Dysfunction in Inflammatory Bowel Disease." *Inflammatory Bowel Diseases* 23: 1718–1729. https://doi.org/10.1097/MIB.0000000000001246.

van der Lelie, D., A. Oka, S. Taghavi, et al. 2021. "Rationally Designed Bacterial Consortia to Treat Chronic Immune-Mediated Colitis and Restore Intestinal Homeostasis." *Nature Communications* 12: 3105. https://doi.org/10.1038/s41467-021-23460-x.

van der Post, S., K. S. Jabbar, G. Birchenough, et al. 2019. "Structural Weakening of the Colonic Mucus Barrier Is an Early Event in Ulcerative Colitis Pathogenesis." *Gut* 68: 2142–2151. https://doi.org/10.1136/gutjnl-2018-317571.

Walrath, T., K. U. Dyamenahalli, H. J. Hulsebus, et al. 2021. "Age-Related Changes in Intestinal Immunity and the Microbiome." *Journal of Leukocyte Biology* 109: 1045–1061. https://doi.org/10.1002/JLB.3RI0620-405RR.

Wang, Q., W. Zhang, J. Liu, W. Qin, and J. Cai. 2025. "Exopolysaccharide of *Levilactobacillus brevis* M-10 Improved Physiological and Biochemical Indicators and Gut Microbiota in DSS-Induced Colitis Mice." *Current Microbiology* 82: 204. https://doi.org/10.1007/s00284-025-04190-5.

Xia, K., R. Gao, L. Li, et al. 2024. "Transformation of Colitis and Colorectal Cancer: A Tale of Gut Microbiota." *Critical Reviews in Microbiology* 50: 653–662. https://doi.org/10.1080/1040841X.2023.2254388.

Xiao, X., X. Mao, D. Chen, et al. 2022. "miRNAs Can Affect Intestinal Epithelial Barrier in Inflammatory Bowel Disease." *Frontiers in Immunology* 13: 868229. https://doi.org/10.3389/fimmu.2022.868229.

Xin, J., L. He, Y. Li, et al. 2025. "Sanguinarine Chloride Hydrate Mitigates Colitis Symptoms in Mice Through the Regulation of the Intestinal Microbiome and Metabolism of Short-Chain Fatty Acids." *Biochimica et Biophysica Acta (BBA)—Molecular Basis of Disease* 1871: 167579. https://doi.org/10.1016/j.bbadis.2024.167579.

Xu, Y.-L., C.-L. Ding, C.-L. Qian, Z.-T. Qi, and W. Wang. 2019. "Retinoid Acid Induced 16 Deficiency Aggravates Colitis and Colitis-Associated Tumorigenesis in Mice." *Cell Death & Disease* 10: 958. https://doi.org/10.1038/s41419-019-2186-9.

Yang, C., and D. Merlin. 2024. "Unveiling Colitis: A Journey Through the Dextran Sodium Sulfate-Induced Model." *Inflammatory Bowel Diseases* 30: 844–853. https://doi.org/10.1093/ibd/izad312.

Yang, F., Y. Su, C. Yan, T. Chen, and P. C. K. Cheung. 2024. "Attenuation of Inflammatory Bowel Disease by Oral Administration of Mucoadhesive Polydopamine-Coated Yeast $\beta$-Glucan via ROS Scavenging and Gut Microbiota Regulation." *Journal of Nanobiotechnology* 22: 166. https://doi.org/10.1186/s12951-024-02434-3.

Yang, J., Y. Xiao, N. Zhao, et al. 2024. "PIM1-HDAC2 Axis Modulates Intestinal Homeostasis Through Epigenetic Modification." *Acta Pharmaceutica Sinica B* 14: 3049–3067. https://doi.org/10.1016/j.apsb.2024.04.017.

Yang, S., and M. Yu. 2021. "Role of Goblet Cells in Intestinal Barrier and Mucosal Immunity." *Journal of Inflammation Research* 14: 3171–3183. https://doi.org/10.2147/JIR.S318327.

Yang, Y., Y. Wang, L. Zhao, et al. 2023. "Chinese Herbal Medicines for Treating Ulcerative Colitis via Regulating Gut Microbiota-Intestinal Immunity Axis." *Chinese Herbal Medicines* 15: 181–200. https://doi.org/10.1016/j.chmed.2023.03.003.

Yao, D., W. Dai, M. Dong, C. Dai, and S. Wu. 2021. "MUC2 and Related Bacterial Factors: Therapeutic Targets for Ulcerative Colitis." *eBioMedicine* 74: 103751. https://doi.org/10.1016/j.ebiom.2021.103751.

Yuan, Y., F. Wang, X. Liu, B. Shuai, and H. Fan. 2023. "The Role of AMPK Signaling in Ulcerative Colitis." *Drug Design, Development and Therapy* 17: 3855–3875. https://doi.org/10.2147/DDDT.S442154.

Zhang, H., Y. Shi, C. Lin, et al. 2023. "Overcoming Cancer Risk in Inflammatory Bowel Disease: New Insights Into Preventive Strategies and Pathogenesis Mechanisms Including Interactions of Immune Cells, Cancer Signaling Pathways, and Gut Microbiota." *Frontiers in Immunology* 14: 1338918. https://doi.org/10.3389/fimmu.2023.1338918.

Zhang, S., H. Wang, and M. J. Zhu. 2019. "A Sensitive GC/MS Detection Method for Analyzing Microbial Metabolites Short Chain Fatty Acids in Fecal and Serum Samples." *Talanta* 196: 249–254. https://doi.org/10.1016/j.talanta.2018.12.049.

Zhang, S., R. Wang, R. Zhao, et al. 2025. "*Alistipes putredinis* Ameliorates Metabolic Dysfunction-Associated Steatotic Liver Disease in Rats via Gut Microbiota Remodeling and Inflammatory Suppression." *Nutrients* 17: 2013. https://doi.org/10.3390/nu17122013.

Zhang, W.-W., K. Thakur, J.-G. Zhang, and Z.-J. Wei. 2024. "Riboflavin Ameliorates Intestinal Inflammation via Immune Modulation and Alterations of Gut Microbiota Homeostasis in DSS-Colitis C57BL/6 Mice." *Food & Function* 15: 4109–4121. https://doi.org/10.1039/d4fo00835a.

Zhang, Y., P. Cao, D. Qin, Y. Zhao, X. Chen, and P. Ma. 2025. "Anti-Inflammatory, Anti-Colitis, and Antioxidant Effects of Columbianadin Against DSS-Induced Ulcerative Colitis in Rats via Alteration of HO-1/Nrf2 and TLR4-NF-$\kappa$B Signaling Pathway." *Inflammopharmacology* 33: 341–352. https://doi.org/10.1007/s10787-024-01630-9.

Zheng, B., H. Wen, B. Zheng, X. Xiang, and C. Zhu. 2025. "Dietary Carbohydrates and the Intestinal Barrier: Emerging Insights Into NF-$\kappa$B Modulation and Health Outcomes." *Journal of Agricultural and Food Chemistry* 73, no. 34: 21264–21282. https://doi.org/10.1021/acs.jafc.5c06354.

Zheng, Y., X. Chen, C. Ding, X. Liu, L. Chi, and S. Zhang. 2024. "Abscisic Acid Ameliorates D-Galactose-Induced Aging in Mice by Modulating AMPK-SIRT1-p53 Pathway and Intestinal Flora." *Heliyon* 10: e28283. https://doi.org/10.1016/j.heliyon.2024.e28283.

Zou, J., C. Liu, S. Jiang, D. Qian, and J. Duan. 2021. "Cross Talk Between Gut Microbiota and Intestinal Mucosal Immunity in the Development of Ulcerative Colitis." *Infection and Immunity* 89: e0001421. https://doi.org/10.1128/IAI.00014-21.

Zuo, T., and S. C. Ng. 2018. "The Gut Microbiota in the Pathogenesis and Therapeutics of Inflammatory Bowel Disease." *Frontiers in Microbiology* 9: 2247. https://doi.org/10.3389/fmicb.2018.02247.